IJMMM International Journal of Minerals, Metallurgy and Materials 矿物冶金与材料学报（英文版）

Recent progress in Ni-rich layered oxides and related cathode materials for Li-ion cells

Boyang Fu, Maciej Modzierz, Andrzej Kulka, and Konrad wierczek

Cite this article as:
Boyang Fu, Maciej Modzierz, Andrzej Kulka, and Konrad wierczek, Recent progress in Ni-rich layered oxides and related cathode materials for Li-ion cells, *Int. J. Miner. Metall. Mater.*, 31(2024), No. 11, pp. 2345-2367. https://doi.org/10.1007/s12613-024-2948-y

---

Articles you may be interested in

Cheng Yang, Jia-liang Zhang, Qian-kun Jing, Yu-bo Liu, Yong-qiang Chen, and Cheng-yan Wang, Recovery and regeneration of $LiFePO_4$ from spent lithium-ion batteries via a novel pretreatment process, *Int. J. Miner. Metall. Mater.*, 28(2021), No. 9, pp. 1478-1487. https://doi.org/10.1007/s12613-020-2137-6

Zhi-yuan Feng, Wen-jie Peng, Zhi-xing Wang, Hua-jun Guo, Xin-hai Li, Guo-chun Yan, and Jie-xi Wang, Review of silicon-based alloys for lithium-ion battery anodes, *Int. J. Miner. Metall. Mater.*, 28(2021), No. 10, pp. 1549-1564. https://doi.org/10.1007/s12613-021-2335-x

Kai-lin Cheng, Dao-bin Mu, Bo-rong Wu, Lei Wang, Ying Jiang, and Rui Wang, Electrochemical performance of a nickel-rich $LiNi_{0.6}Co_{0.2}Mn_{0.2}O_2$ cathode material for lithium-ion batteries under different cut-off voltages, *Int. J. Miner. Metall. Mater.*, 24(2017), No. 3, pp. 342-351. https://doi.org/10.1007/s12613-017-1413-6

Liu-ye Sun, Bo-rui Liu, Tong Wu, Guan-ge Wang, Qing Huang, Yue-feng Su, and Feng Wu, Hydrometallurgical recycling of valuable metals from spent lithium-ion batteries by reductive leaching with stannous chloride, *Int. J. Miner. Metall. Mater.*, 28(2021), No. 6, pp. 991-1000. https://doi.org/10.1007/s12613-020-2115-z

Qiao-kun Du, Qing-xia Wu, Hong-xun Wang, Xiang-juan Meng, Ze-kai Ji, Shu Zhao, Wei-wei Zhu, Chuang Liu, Min Ling, and Cheng-du Liang, Carbon dot-modified silicon nanoparticles for lithium-ion batteries, *Int. J. Miner. Metall. Mater.*, 28(2021), No. 10, pp. 1603-1610. https://doi.org/10.1007/s12613-020-2247-1

Qi Wang, Yue-yong Du, Yan-qing Lai, Fang-yang Liu, Liang-xing Jiang, and Ming Jia, Three-dimensional antimony sulfide anode with carbon nanotube interphase modified for lithium-ion batteries, *Int. J. Miner. Metall. Mater.*, 28(2021), No. 10, pp. 1629-1635. https://doi.org/10.1007/s12613-021-2249-7

IJMMM WeChat

QQ author group

INTERNATIONAL JOURNAL OF
Minerals, Metallurgy and Materials

Volume 31, Number 11, November 2024
Page 2345

Review

https://doi.org/10.1007/s12613-024-2948-y

Recent progress in Ni-rich layered oxides and related cathode materials for Li-ion cells

Boyang Fu[1)], *Maciej Moździerz*[1)], *Andrzej Kulka*[1,2)], *and Konrad Świerczek*[1,2),✉]

1) Faculty of Energy and Fuels, AGH University of Krakow, al. A. Mickiewicza 30, 30-059 Krakow, Poland
2) AGH Centre of Energy, AGH University of Krakow, ul. Czarnowiejska 36, 30-054 Krakow, Poland
(Received: 23 March 2024; revised: 27 May 2024; accepted: 31 May 2024)

Abstract: Undoubtedly, the enormous progress observed in recent years in the Ni-rich layered cathode materials has been crucial in terms of pushing boundaries of the Li-ion battery (LIB) technology. The achieved improvements in the energy density, cyclability, charging speed, reduced costs, as well as safety and stability, already contribute to the wider adoption of LIBs, which extends nowadays beyond mobile electronics, power tools, and electric vehicles, to the new range of applications, including grid storage solutions. With numerous published papers and broad reviews already available on the subject of Ni-rich oxides, this review focuses more on the most recent progress and new ideas presented in the literature references. The covered topics include doping and composition optimization, advanced coating, concentration gradient and single crystal materials, as well as innovations concerning new electrolytes and their modification, with the application of Ni-rich cathodes in solid-state batteries also discussed. Related cathode materials are briefly mentioned, with the high-entropy approach and zero-strain concept presented as well. A critical overview of the still unresolved issues is given, with perspectives on the further directions of studies and the expected gains provided.

Keywords: lithium-ion batteries; cathode materials; nickel-rich layered oxides; recent progress; critical issues; improvement strategies

1. Introduction

Since their introduction to the market by Sony Corporation in 1991, lithium-ion batteries (LIBs) have become the dominant power source in portable electronics and power tools. Nowadays, LIBs hold a dominant position also in the electric vehicles (EVs) market, as well as their application in the emerging stationary electrical energy storage systems is growing very fast. Obviously, electrification of transportation and other sectors, which is currently understood as the most promising solution to address the urgent energy and environmental challenges associated with fossil fuels consumption, has become one of the driving forces behind the spectacular commercial success of LIBs [1–3]. Nevertheless, there is still a constant need to develop better batteries, which exhibit improved useful properties and safety, are cheaper, and can be used for a longer time in different environmental conditions.

It is generally considered that a cathode limits electrochemical performance, and consequently, in order to achieve the driving range of EVs significantly exceeding 500 kilometers, the development of the high energy-density cathode materials is imperative. The initially used $LiCoO_2$ layered oxide does not allow achieving the desired functional parameters, due to the relatively low reversible capacity. Also, the usage of Co is burdened by serious issues, including environmental pollution and high costs [4]. Interestingly, the Ni-based alternative, $LiNiO_2$, with much higher capacity (>200 $mAh \cdot g^{-1}$) and similar operating voltage vs. Li/Li^+, was proposed by Dahn *et al.* as early as in the 1990s [5], but strong limitations troubling that material were soon recognized. Among them, the instability issues associated, i.a., with the cation mixing of Li^+ and Ni^{2+}, complex Li–Ni–O phase diagram features with a tendency to form off-stoichiometric compounds, insufficient thermal stability, as well as degradation and problematic oxygen release at highly-charged states, should be mentioned. It can be stated that two of the most commonly considered series of layered cathode materials, $LiNi_{1-x-y}Co_xMn_yO_2$ (NCM) and $LiNi_{1-x-y}Co_xAl_yO_2$ (NCA), are in fact oxides in which high capacity of the $LiNiO_2$ end-member was partially sacrificed by Co–Mn or Co–Al doping to ensure stable and safe operation [6–7].

Regarding the historical development of Ni-rich layered oxides, one of the most notable compositions is $LiNi_{0.33}Co_{0.33}Mn_{0.333}O_2$ (NCM111), proposed by Ohzuku and Makimura in 2001 [8]. Numerous papers have been published afterwards, and a general trend can be observed that more and more Ni could be successfully introduced, yielding enhanced electrochemical performance. Concurrently, the usage of cobalt has been strongly reduced, starting from $LiNi_{0.6}Co_{0.2}Mn_{0.2}O_2$ (NCM622) [9–12], $LiNi_{0.8}Co_{0.15}Al_{0.05}O_2$ (NCA81505, Tesla Model S) [13], and $LiNi_{0.8}Co_{0.1}Mn_{0.1}O_2$

✉ Corresponding author: Konrad Świerczek E-mail: xi@agh.edu.pl

(NCM811) [14–22], up to Co-free materials developed recently [23–34]. The interest in further development of those materials remains high, as can be inferred from Web of Science database queries presented in Fig. 1.

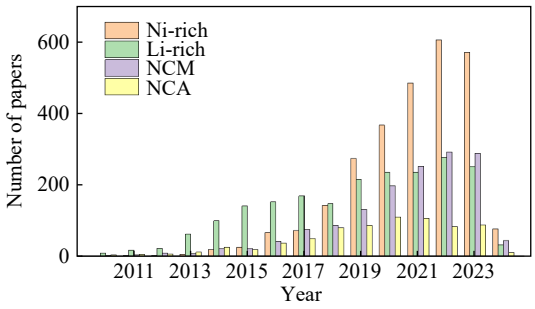

Fig. 1. Search results in the Web of Science database (conducted on March 15th 2024) on "Ni-rich cathodes", "Li-rich cathodes", "NCM cathodes", "NCA cathodes". Results for the alternative "NMC cathodes" name are slightly lower, comparing to the NCM, and are not shown.

Naturally, a number of review papers are also available, with the authors discussing different, important aspects related to the Ni-rich cathode materials. This includes suggested directions for the further development of Co-less Ni-rich cathodes [35], a discussion about performance fading mechanisms and modification strategies [36], an overview of the progress on electrolyte functional additives, especially designed for Ni-rich cathodes [37], and the presentation of strategies to improve performance, with, i.a., primary particles engineering methods [38]. Cost and performance analyzes, as well as challenges and solutions for Co-free and Co-poor NCM materials, are also summarized [39]. Other authors focus more on aspects related to structural evolution during cycling and its impact on electrochemical performance [40]. A general overview of different issues and proposed solutions is also available, which, among others, provides data on residual lithium compounds, cation mixing, oxygen loss, and microcracking [41]. With the growing interest in the use of computational methods in the development of cathode materials, comprehensive review on this topic is also available, with sections covering important NCM and NCA compositions, as well as respective surface coating and doping studies [42]. Several reviews have recently been published, summarizing current knowledge on the degradation mechanisms and the corresponding mitigation strategies [43], reduction of microcracks [44–45], thermal stability, and outgassing of Ni-rich cathodes [45]. A very comprehensive overview of various doping approaches is also published [43,46]. All of the discussed papers indicate that while Ni-rich cathodes are indeed very attractive, due to the possibility of achieving very high energy-density values, there are still serious, unresolved problems related to their long-term stability and degradation, thermal stability and safety, electrolyte compatibility, as well as scalability and costs of production. Following the concept presented by Yang *et al.* in Ref. [43], the issues related to Ni-rich materials can be divided into two main groups of the surface degradation and mechanical failure, with more specific, but interrelated problems being identified (Fig. 2). The next chapter is devoted to discussing those issues in more details.

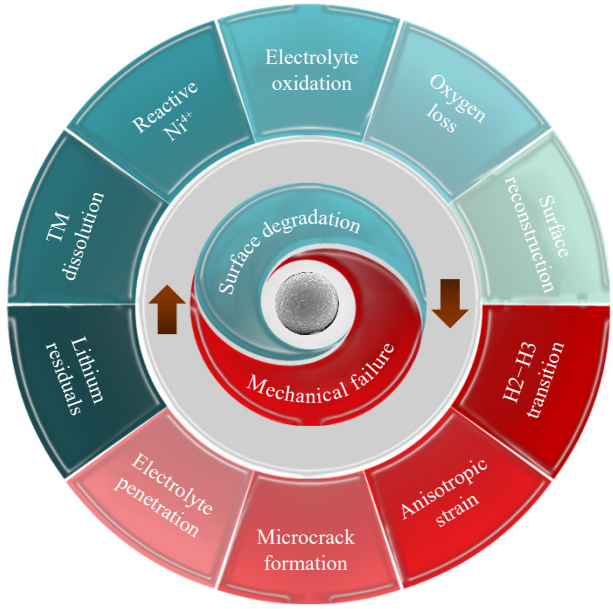

Fig. 2. Main identified issues contributing to the capacity fading of Ni-rich cathodes used in LIBs. The figure is based on the concept presented by Yang *et al.* [43]. TM: transition metal. H2 and H3 correspond to the respective phases present at the highly-charged state [40]. Adapted from *Energy Storage Mater.*, Vol. 63, J. Yang, X.H. Liang, H.H. Ryu, C.S. Yoon, and Y.K. Sun, Ni-rich layered cathodes for lithium-ion batteries: From challenges to the future, 102969, Copyright 2023, with permission from Elsevier.

With a summary of papers covering a broad range of topics being already available, this review focuses more on the most recent progress and new ideas presented in the literature concerning the overcoming of the intrinsic problems occurring in the Ni-rich cathodes. After discussing the crucial issues contributing to the capacity fade (Section 2), the following chapters present selected data on doping and composition optimization, including novel multicomponent approaches and studies directed at the development of zero-strain cathodes. With advancements related to the introduction of the so-called high-entropy oxides, Li-rich cathode materials are also mentioned. Other chapters contain references to advanced coating strategies with multifunctional protection layers. Concentration gradient and single crystal materials, as well as several innovations concerning electrolytes and their modification, are also discussed. In addition, the possibility of the application of Ni-rich cathodes in solid-state batteries is briefly presented. Finally, a short critical overview of the still unresolved issues is given, with most promising perspectives and possible further directions of the relevant studies being also provided.

2. Degradation mechanisms of Ni-rich layered cathodes

It is already established that the degradation mechanisms

of Ni-rich layered cathodes can be mainly attributed to two reasons [36,43]: one is associated with the surface structure degradation, and the other one comes from the mechanical failure. Those effects lead to the insufficient cycle life (capacity decay) of such cathodes, but also contribute to the poor thermal stability, which brings safety risks, hindering further expansion in the market.

2.1. Surface degradation

(1) Lithium residuals.

Obviously, the volatilization of Li is taken into consideration during the synthesis process of Ni-rich oxides. Usually, a particular excess of Li is required to produce a highly-ordered layered structure, which inevitably brings issues with residual lithium on the surface of the active material particles, mainly comprising LiOH and Li_2CO_3 [47]. Studies have shown that this residual lithium not only causes polyvinylidene difluoride (PVDF) gelation during the slurry preparation process, but also hinders the diffusion of lithium ions during the electrochemical cycling, causing capacity decay [48–49].

(2) TM dissolution.

Issues associated with transition metal (TM) dissolution contribute significantly to the degradation of performance of the high nickel content materials. This dissolution primarily occurs due to the erosion caused by hydrofluoric acid (HF), which is previously formed by the hydrolysis of $LiPF_6$ in the electrolyte [50]. Moreover, the solubility of low-valent metal ions exceeds that of the high-valent metal ions in the electrolyte, facilitating the dissolution of low-valent transition metal oxides, formed by the oxygen loss (at the charged state). Consequently, TM dissolution leads to a reduction in lithium-ion insertion sites, resulting in the capacity and voltage decay. Additionally, dissolved metal ions migrate to the negative electrode surface, where they participate in the formation of the solid electrolyte interphase film (SEI), thereby increasing impedance, and contributing to the battery performance degradation [51].

(3) Reactive Ni^{4+}.

The higher nickel content in Ni-rich materials contributes to the higher specific capacity, because the active $Ni^{2+/3+}$ can be fully oxidized to Ni^{4+} during the cathode delithiation process, to maintain the charge balance [52]. However, highly-active Ni^{4+} cations are prone to the side reactions with the electrolyte, leading to a decomposition of the electrolyte and also, degradation of the Ni-rich cathode surface. Consequently, the increase in the Ni^{4+} content reduces the cycle stability and thermal stability of the Ni-rich oxides [53].

(4) Electrolyte oxidation.

It is elaborated that the electrolyte decomposition involves electrochemical and chemical oxidation pathways, among which chemical oxidation is the main pathway for the electrolyte decomposition, while the active surface of the charged cathode causes chemical oxidation of the electrolyte [54]. Oxidation of the electrolyte will not only release gaseous products, but also generate solid products, cause an increase in the thickness of the cathode electrolyte interphase (CEI) on the cathode surface, hinder lithium-ion transmission, and increase interface impedance, thereby causing capacity fade during long-term cycling [55]. The discussed above large amount of Ni^{4+} in a highly charged state increases the reactivity of the cathode surface and the electrolyte. The harmful side reactions between the two will cause the capacity of the Ni-rich cathode to decay, which will intensify as the nickel content increases [56].

(5) Oxygen loss.

At the end of charging, the layered cathode, in a highly delithiated state, will release oxygen, which is due to the structural/electronic instability (see also Section 3). As the Ni content increases, the potential of the oxygen evolution becomes lower and lower. For example, for the NCM111 and NCM811 cathodes, the values are 4.6 and 4.2 V, respectively [57]. In addition, the starting temperature of the cathode structural transformation and oxygen release are also affected by the state of charge (SOC). The higher the SOC, the lower the starting temperature of the transformation and the higher is amount of released oxygen. In batteries, oxygen release will not only cause the deterioration of the cathode structure, but may also lead to the thermal runaway under even a relatively low charge state, which is a key cause of safety hazards [58].

(6) Surface reconstruction.

In layered oxides, low-valent metal cations may migrate to the Li^+ ion layer, and occupy the structural position of Li^+ ions. Among them, Ni^{2+} (low spin, octahedral site, 0.69 Å) and Li^+ (0.76 Å) have similar ionic radii, so they exhibit the strongest mixing tendency. Ni/Li mixing and the oxygen evolution discussed above may lead to the transformation of the layered phase to the spinel rock salt phase [59]. Consequently, the NiO rock salt phase layer (formed in the near surface regions), which has neither electrochemical activity nor ionic conductivity, is considered to be one of the main reasons for the deterioration of the electrochemical performance of the Ni-rich cathodes [59–60]. At the same time, this transformation will also intensify with the nickel content and SOC increase.

2.2. Mechanical failure

(1) H2–H3 phase transition.

Ni-rich materials essentially follow the solid solution mechanism during the electrochemical cycling, and like their parent material, $LiNiO_2$ (LNO), they show a series of phase changes of H1 → M → H2 → H3 on charge (although visibility of such changes, especially presence of the monoclinic phase, depends on the actual chemical composition of the material) [40,61]. Among the structural transformations, it is observed that during the H2–H3 phase transition, the lattice parameter *c* decreases strongly, which can lead to severe mechanical degradation. By studying the mechanical properties of LNO under different cut-off voltages, it was found that the H2–H3 phase transition is the main cause of formation of microcracks [62]. At the same time, the starting voltage of H2–H3 phase transition decreases with the increase of nickel content [63]. It should be mentioned that in order to obtain a

high capacity, it is necessary to charge the material to the point of this phase transition.

(2) Anisotropic strain.

As previously elucidated, the transition from the H2 to H3 phase causes a sudden change in the *c*-axis lattice parameter. With the emergence of the H3 phase, that change causes the lattice volume to decrease slowly first, and then, drop suddenly. During the delithiation process the change is more abrupt along the *c*-axis direction than in the *a*-axis direction. Such anisotropic change causes the accumulation of stresses at the grain boundaries, thereby inducing the formation of microcracks within the secondary particles [64]. At the same time, the concentration gradient and lithium vacancies generated when Li^+ diffuses out of the layered structure, the relatively low spatial interconnectivity of the conductive carbon and binder in the cathode, as well as the overpotential caused by the high charging rate, all lead to the Li^+ dissipation between the primary particles, and to their uneven distribution throughout the cathode. This further exacerbates the anisotropic lattice shrinkage during charging, resulting in the formation of microcracks at the grain boundaries [65].

(3) Microcracks formation.

Microcracking is generally considered to be the result of the mechanical strain induced by the anisotropic lattice volume changes during cycling. Microcracks tend to nucleate and propagate at the grain boundaries and lattice defects within the grains (primary particles). The secondary particles of the Ni-rich layered cathode materials are generally spherical, and are composed of randomly oriented and dense-arranged primary particles. Since the stresses inside the secondary particles have anisotropic characteristics, they accumulate at the grain boundaries, causing microcracks to generate and develop, expanding to the surface of the secondary particles, seriously crushing the entire secondary particles [66]. Generally, the amount of microcracks produced in Ni-rich materials increases with the increase of Ni content, SOC, and temperature [67]. This is consistent with the role of the H2–H3 phase transition, analyzed in the previous sections.

(4) Electrolyte penetration.

Once the microcracks inside the secondary particles spread to the surface, they provide channels for the electrolyte to penetrate into the interior of the secondary particles. Consequently, they accelerate the degradation of the exposed surface inside the particles, enrich with the NiO rock salt phase and solid electrolyte decomposition products on the microcracks surface, and hinder the interfacial Li^+ transport [67]. This not only causes the impedance to increase, the battery capacity and the operating voltage to decrease, but also intensifies the gas production of the battery, further increasing the probability of the battery thermal runaway, and causing safety hazards [68].

3. Doping and composition optimization

It is considered that differences in the (de-)lithiation behavior of $LiCoO_2$ and $LiNiO_2$ originate mainly from a different electronic structure of both compounds. The oxidation of Ni^{3+} (low spin $t_{2g}^6e_g^1$) to Ni^{4+} (t_{2g}^6) is easier in comparison to the change from Co^{3+} (low spin t_{2g}^6) to Co^{4+} (t_{2g}^5), as electrons can be removed more easily from e_g orbital [69]. Consequently, Ni-rich layered materials exhibit higher capacity, and there are less problems with oxygen loss at higher charge states. Nevertheless, because of the Jahn-Teller effect associated with Ni^{3+}, there are strong distortions present, which result in the structural instability during the electrochemical cycling [70]. Also, Ni^{2+} is not easily oxidized (during the synthesis process), and exhibits similar ionic radius in comparison to Li^+ in the octahedral coordination. This gives rise to the cation mixing effect, which is detrimental for the ionic transport [71]. In the well-established NCM and NCA series, especially for oxides with high Ni content, the reversible capacity is linked with the redox process of nickel. The main role of Co is to limit the Li/Ni mixing, while stable Mn or Al cations contribute to the improved stability [72–74]. However, numerous published results indicate that the properties of those materials can be further optimized by a proper introduction of various other elements. As presented in the review paper [46], dopants can be classified according to their formal charge. For example, if relatively large Na^+ is introduced into the Li sites of Ni-rich materials as a pillar ion, it enlarges the Li layer, resulting in improved electrochemical characteristics, especially, rate performance [75–79]. Doping with +2 cations can also have a positive influence, particularly in reducing the diffusion barrier for lithium transport [80–81], and improving structural stability [82]. Among the typically studied dopants, Ca^{2+} [83–84], Mg^{2+} [85–86], and Zn^{2+} [87] should be mentioned. Interestingly, e.g., Ca^{2+} and Mg^{2+} can occupy Li and TM sites simultaneously. This may cause complex behavior, as magnesium present at 3b sites is prone to destabilization at highly-charged states [88–89]. However, Mg^{2+} cations present at the lithium sites play a stabilizing role through the pillar effect [90]. There is, in fact, an ongoing discussion on the actual role of the Mg, concerning stability or the prevention of microcrack formation originating from the H2–H3 phase transition [61,91]. Apart from the well-proven stabilizing role of Al^{3+} [74], doping with the electrochemically-active Cr^{3+} is also considered [92–93]. The introduction of B^{3+}, occupying rather tetrahedral (empty) sites [94–95], may help mitigate volume changes and the formation of microcracks on cycling through the morphology changes of the primary particles arrangement in the grains [96]. The obvious dopant, Co^{3+}, is crucial to reduce the Li/Ni mixing, but is also important for thermal stability [97]. However, it should be emphasized that the development of Co-free Ni-rich materials is now considered as the main direction for further development of the LIB cathodes. It is also important to notice rather an obvious, but sometimes omitted conclusion, that practically in all cases, only a proper concentration of a particular dopant gives positive results, while too small or too high amount causes worsening of various properties. The introduction of high-valence cations has been studied as well, and often such ions are introduced as co-

dopants to different NCA or NCM materials. Since in many cases the solid solution levels are not high, or there are other more complex phenomena that occur, with a proper concentration of the modifier, apart from pure doping, simultaneous doping/coating may also take place [98–100]. Among the high-valence dopants, Ce^{4+} [101], Sn^{4+} [102], Zr^{4+} [103], Hf^{4+} [104], Mn^{4+} [105], Nb^{5+} [100], Ta^{5+} [106], V^{5+} [107], W^{6+} [108], and Mo^{6+} [109], should be mentioned as the most promising and studied.

Since doping of the Ni-rich cathode materials has undergone extensive examination, distinct mechanisms have been recognized and linked to the improvement of the properties. As presented by Cui *et al.* [46] (Fig. 3), the beneficial role is usually linked with improved structural and chemical stability through the introduction of stronger dopant-oxygen bonds, a lower level of Li/Ni mixing, prevention of structural collapse, but also, the mitigation of strain and microcracks formation. Finally, some of the dopants can modify the structure of the particles as well (doping/coating), providing additional protection. In many cases, an accelerated Li^+ diffusion can be also observed, as well as the interfacial stability is improved. Obviously, selection criteria for the successful dopant should include solubility limits, preferred doping site in the crystal structure, possible segregation, electrochemical activity, etc. While there is usually a tradeoff between the performance and stability, a balanced doping can be indeed very beneficial. Interested reader can find comprehensive discussion about effects of dopants and the corresponding mechanism of their work for different considered elements in the mentioned review paper by Cui *et al.* [46].

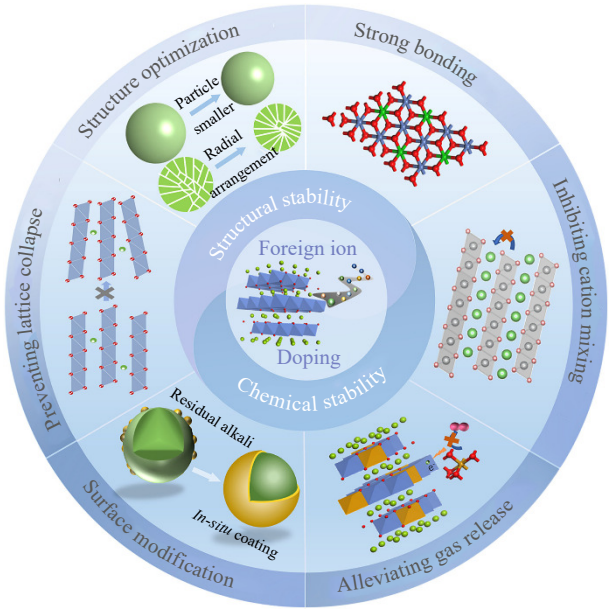

Fig. 3. Action mechanism of element doping [46]. Reprinted from *Energy Storage Mater.*, Vol. 57, Z.Z. Cui, X. Li, X.Y. Bai, X.D. Ren, and X. Ou, A comprehensive review of foreign-ion doping and recent achievements for nickel-rich cathode materials, 14-43, Copyright 2023, with permission from Elsevier.

Noteworthy results could be obtained for doping with Mg of the high Ni-content NMC materials, with the aim to overcome instability problems at reasonable costs. Gomez-Martin *et al.* [110] investigated a series of Mg-substituted NMC materials with 90mol% Ni regarding key performance metrics in full-cells with the graphite anode (tested in the range of 2.9–4.2 V). $LiNi_{0.80}Mn_{0.10}Co_{0.10}O_2$, $LiNi_{0.90}Mn_{0.05}Co_{0.05}O_2$, and different Mg-doped samples were synthesized using the same co-precipitation route. It was found that the use of 1mol%–2mol% Mg improved the key parameters (specific energy, cycle life), with the added advantage of the decreased Co content (Fig. 4(a)).

In order to address the swift degradation observed at high voltages, Sun *et al.* [111] employed antimony as a dopant (less commonly used). The objective of the research was to mitigate the lattice instability within the high Ni-content layered structure, with a particular focus on the grain boundary regions. Those regions are crucial as they are prone to degradation, and serve as points of concentration for deterioration at the cathode–electrolyte interfaces. The resulting $LiNi_{0.895}Co_{0.05}Mn_{0.05}Sb_{0.05}O_2$ cathode was found to deliver stable cycling performance despite the 3 h dwell time at the charged state, as compared with the undoped $LiNi_{0.90}Co_{0.05}Mn_{0.05}O_2$ (37.5% vs. 90.8% capacity retention after 100 cycles, respectively) (Fig. 4(b)). Additionally, the modified electrode demonstrated improved stability (Fig. 4(c)–(f)) and fast charging capability, achieving a discharge capacity of 216.7 $mAh \cdot g^{-1}$ (as compared to 197.0 $mAh \cdot g^{-1}$ for the undoped counterpart) at a 4 C charge rate.

In another recent work, Wang *et al.* [104] explored a viable Hf-doping method to improve the electrochemical performance of $LiNi_{0.9}Co_{0.08}Al_{0.02}O_2$. The introduction of a small amount of Hf (0.5mol%) resulted in the refinement of the primary particles, transforming them into a compact, short rod shape, and arranged densely along the radial direction. This configuration increased the toughness of the secondary particles, while reducing the internal porosity. Additionally, Hf-doping played a beneficial role in stabilizing the layered structure and suppressing side reactions by the introduction of robust Hf–O bonds (Fig. 5). As expected, the Hf-modified cathode was found to deliver an improved reversible capacity retention of 95.3% after 100 cycles at 1 C, as compared with only 82.0% for the unmodified reference material.

Interestingly, Mo substitution has been shown to be a surprisingly useful strategy to enhance the electrochemical stability of Ni-rich Co-free cathode materials, according to Park *et al.* [112]. If properly conducted, Mo-doping results in a refinement of the grain size, effectively alleviating the detrimental strain (caused by the sudden lattice contraction at high voltages) through mechanisms such as fracture toughening and the elimination of localized compositional inhomogeneities. The presence of Mo^{6+} induces enhanced cation ordering, contributing to the stabilization of the delithiated structure through the pillar effect discussed above. Compared to pristine samples and similar cathode materials doped with Co, Al, Ti, Nb, Ta, and W, the introduction of 1mol% Mo into $LiNi_{0.9}Mn_{0.1}O_2$ enabled reaching a capacity of 234 $mAh \cdot g^{-1}$ (charge up to 4.4 V, 0.1 C), as well as affected the voltage of

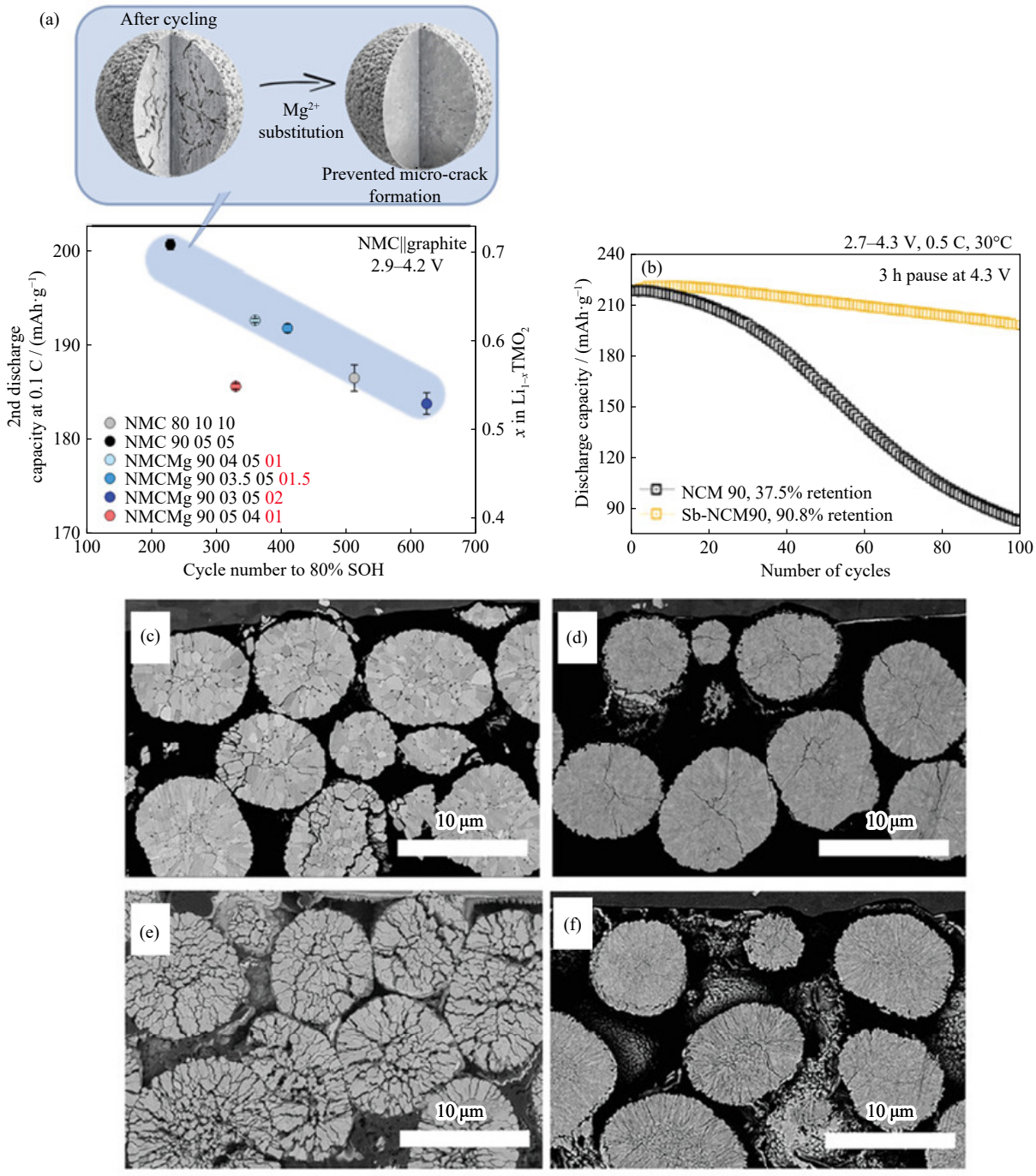

Fig. 4. (a) 2nd discharge specific capacity at a rate of 0.1 C against the attainable cycle numbers to 80% state-of-health (SOH) in NMC||graphite full-cells. The SOH is based on the delivered capacity in the fifth cycle for all materials (1st cycle at 0.33 C). Cell voltage range: 2.8–4.2 V, N/P-ratio: 1.15:1.00, electrolyte: 1 M $LiPF_6$ in 3:7 (vol%) EC/EMC + 2wt% VC. (b) Cycling performance of NCM90 (black) and Sb-NCM90 (gold) with the 3 h pause at the charged state. Cross-sectional scanning electron microscope (SEM) images at the 100th cycles within the 2.7–4.3 V voltage window a 0.5 C-rate: (c) NCM90 without 3 h dwell time at charged state, (d) Sb-NCM90 without 3 h dwell time at charged state, (e) NCM90 with 3 h dwell time at charged state, and (f) Sb-NCM90 with 3 h dwell time at charged state [111]. Used abbreviations are explained in the respective original references. (a) Reprinted from Ref. [110]. (b–f) H.H. Sun, T.P. Pollard, O. Borodin, K. Xu, and J.L. Allen, *Adv. Energy Mater.*, vol. 13, 2204360 (2023) [111]. Copyright Wiley-VCH Verlag GmbH & Co. KGaA. Reproduced with permission.

the H2–H3 transition and improved other electrochemical properties. Also, the cycling stability of a full cell incorporating the optimized $LiNi_{0.89}Mn_{0.1}Mo_{0.01}O_2$ cathode retained 86% of its initial capacity after 1000 cycles.

In another paper, Zhang *et al.* [113] employed a one-step high-temperature solid-phase sintering approach to create a Ta_2O_5 protective layer on the surface of $LiNi_{0.8}Co_{0.15}Al_{0.05}O_2$, with a simultaneous effect of Ta^{5+} incorporation into (near-surface regions of) the lattice, thereby achieving a dual effect of coating and doping (Fig. 6(a)–(f)). The created protective coating effectively inhibited undesired side reactions between the electrode material and the electrolyte, while Ta^{5+}

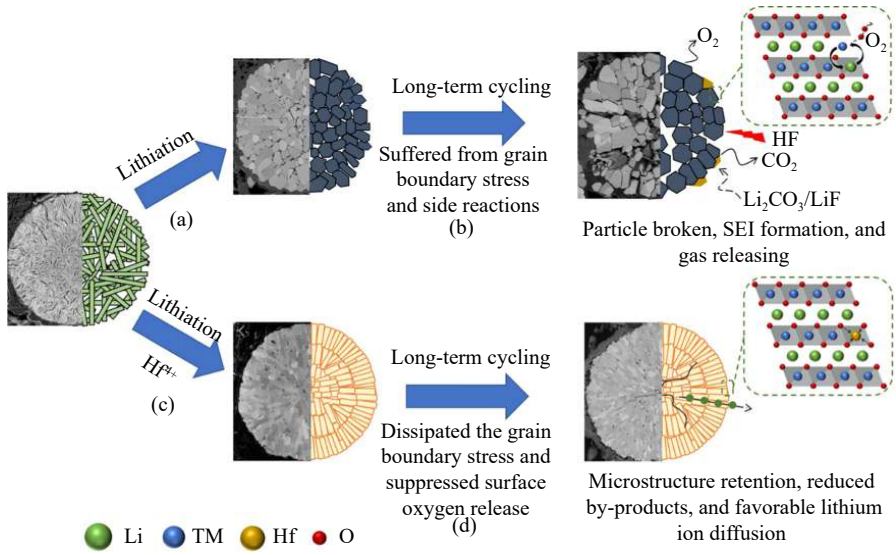

Fig. 5. Schematic diagram of hafnium doping to enhance cycling stability of the Ni-rich NCA: (a, c) lithiation process and (b, d) long-term cycling of the NCA and NCA90-Hf0.5 cathode particles, respectively. Reprinted with permission from B. Wang, F.P. Cai, C.X. Chu, *et al.*, *ACS Appl. Mater. Interfaces*, vol. 16, 12599-12611 (2024) [104]. Copyright 2024 American Chemical Society.

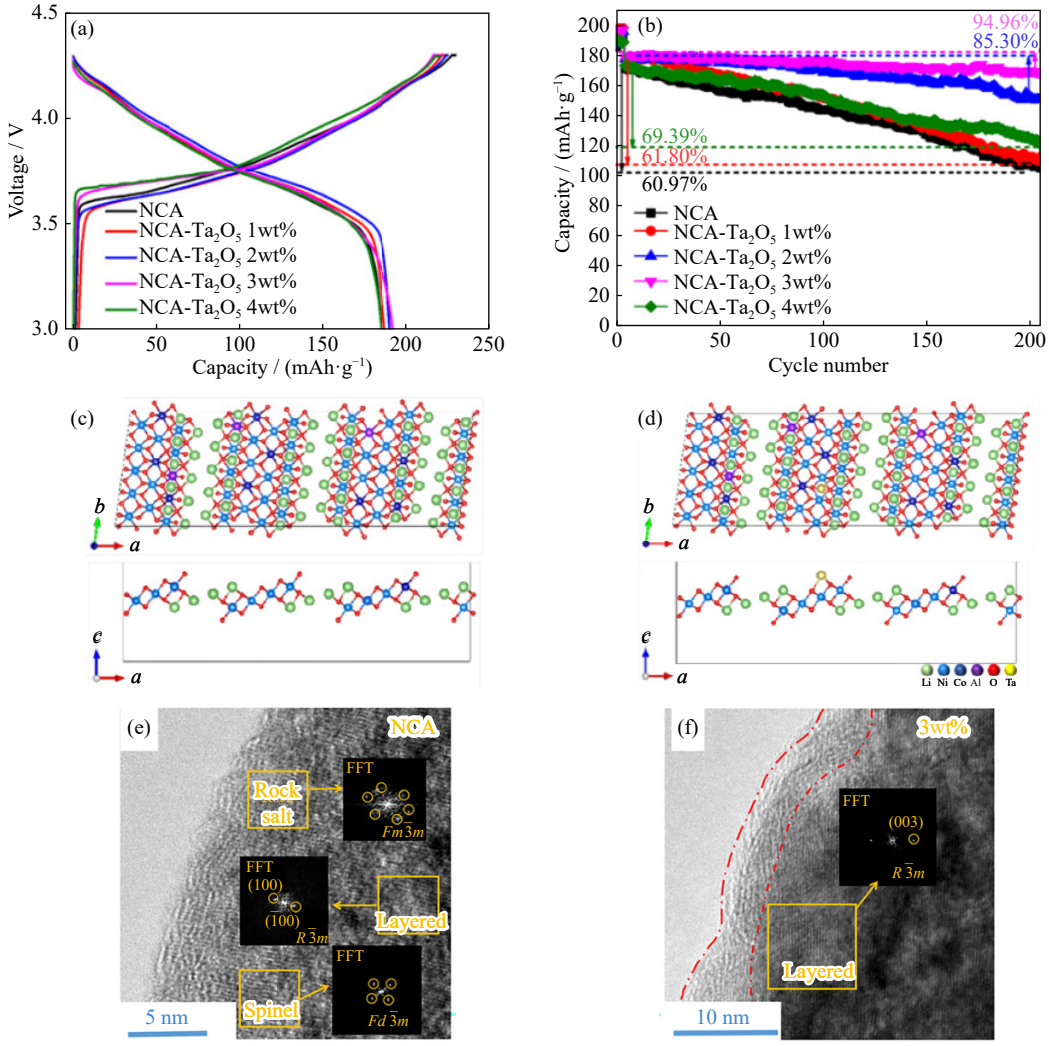

Fig. 6. Electrochemical performance of samples in the voltage range of 3.0–4.3 V: (a) charge and discharge curves for the first cycle; (b) cycle test curves. Top and side views of the models of the NCA (104) surface (c) without and (d) with Ta^{5+} doping. The Li, Ni, Co, Al, O, and Ta atoms are presented by green, blue, dark blue, purple, red, and yellow, respectively. Transition electron microscopy (TEM) with fast Fourier transform (FFT) images for (e) NCA and (f) 3wt% NCA-Ta_2O_5 after 200 cycles. Reprinted with permission from X.Y. Zhang, P.P. Zhang, T.Y. Zeng, *et al.*, *ACS Appl. Energy Mater.*, vol. 4, 8641-8652 (2021) [113]. Copyright 2021 American Chemical Society.

doping alleviated the Li/Ni disorder ratio, significantly enhancing structural stability. The resulting Ta-modified material was found to demonstrate a very good capacity retention of 94.46% at 1 C after 200 cycles, exceeding the 60.97% observed for the pristine sample. The analysis of the structural evolution revealed that the optimized sample maintained a well-preserved spherical structure, without evident cracks, after 200 cycles at 1 C. Furthermore, such electrode showed an exceptional discharge capacity of 151.02 $mAh \cdot g^{-1}$ at a high rate of 10 C.

Finally, data on the electrochemical performance of selected Ni-rich materials and their modified counterparts, as presented in the recent papers, are included for an easy comparison in Table 1 below.

Table 1. Effect of doping with different elements on the electrochemical properties of selected Ni-rich materials

Doping element	Composition before/after doping	Temperature / °C	Voltage range / V	1st discharge capacity before/after doping / ($mAh \cdot g^{-1}$)	Capacity retention before/after doping / %	Ref.
F	$LiNi_{0.5}Co_{0.2}Mn_{0.3}O_2$/$LiNi_{0.5}Co_{0.2}Mn_{0.3}O_{1.99}F_{0.01}$	RT	2.5–4.3	181.44/177.38 (0.1 C)	44.62/75.40 (400 cycles, 2 C)	[114]
Na	$LiNi_{0.8}Co_{0.1}Mn_{0.1}O_2$/$Li_{0.99}Na_{0.01}Ni_{0.8}Co_{0.1}Mn_{0.1}O_2$	25	2.8–4.3	194.4/191.6 (0.1 C)	93.2/96.8 (200 cycles, 1 C)	[77]
K	$LiNi_{0.8}Co_{0.1}Mn_{0.1}O_2$/$Li_{0.99}K_{0.01}Ni_{0.8}Co_{0.1}Mn_{0.1}O_2$	25	2.8–4.3	194.4/194.1 (0.1 C)	93.2/88.7 (200 cycles, 1 C)	[77]
Rb	$LiNi_{0.8}Co_{0.1}Mn_{0.1}O_2$/$Li_{0.99}Rb_{0.01}Ni_{0.8}Co_{0.1}Mn_{0.1}O_2$	25	2.8–4.3	194.4/191.4 (0.1 C)	93.2/92.9 (200 cycles, 1 C)	[77]
Ca	$LiNi_{0.85}Mn_{0.10}Al_{0.05}O_2$/$LiNi_{0.845}Mn_{0.10}Al_{0.05}Ca_{0.005}O_2$	25	2.7–4.3	198.8/196.6 (0.1 C)	89.2/94.9 (200 cycles, 1 C)	[83]
Mg	$LiNi_{0.8}Co_{0.1}Mn_{0.1}O_2$/$Li(Ni_{0.8}Co_{0.1}Mn_{0.1})_{0.97}Mg_{0.03}O_2$	25	3.0–4.5	191.8/226.1 (0.1 C)	67/81 (350 cycles, 0.5 C)	[115]
Zn	$LiNi_{0.94}Co_{0.06}O_2$/$LiNi_{0.94}Co_{0.04}Zn_{0.02}O_{1.99}$	25	2.8–4.4	232/225 (0.1 C)	97.1/99.4 (130 cycles, 1/3 C)	[116]
Al	$LiNi_{0.9}Co_{0.05}Mn_{0.05}O_2$/$LiNi_{0.89}Co_{0.05}Mn_{0.05}Al_{0.01}O_2$	30	2.7–4.3	229/228 (0.1 C)	87.7/90.6 (100 cycles, 0.5 C)	[74]
B	$LiNi_{0.6}Co_{0.2}Mn_{0.2}O_2$/$Li_{1.104}Ni_{0.6}Co_{0.2}Mn_{0.194}B_{0.017}O_2$	RT	3.0–4.3	173.6/188.2 (0.1 C)	73.24/85.96 (200 cycles, 1 C)	[94]
Cr	$LiNi_{0.8}Co_{0.1}Mn_{0.1}O_2$/$LiNi_{0.79}Co_{0.1}Mn_{0.1}Cr_{0.01}O_2$	RT	2.7–4.3	97/104 (10 C)	76.1/89 (50 cycles, 5 C)	[93]
Ce	$Li_{1.2}Mn_{0.54}Ni_{0.13}Co_{0.13}O_2$/$Li(Li_{0.2}Mn_{0.54}Ni_{0.13}Co_{0.13})_{0.995}Ce_{0.005}O_2$	RT	2.0–4.8	196.1/192.7 (1 C)	73.3/98.2 (100 cycles, 1 C)	[101]
Sn	$LiNi_{0.9}Co_{0.05}Mn_{0.05}O_2$/$LiNi_{0.897}Co_{0.05}Mn_{0.05}Sn_{0.003}O_2$	30	2.7–4.3	231/229 (0.1 C)	87.1/92.9 (100 cycles, 0.5 C)	[102]
Zr	$LiNi_{0.95}Co_{0.03}Mn_{0.02}O_2$/$LiNi_{0.948}Co_{0.03}Mn_{0.02}Zr_{0.002}O_2$	25	3.0–4.3	188.5/184.4 (1 C)	60.8/71.3 (250 cycles, 1 C)	[103]
Hf	$LiNi_{0.9}Co_{0.08}Al_{0.02}O_2$/$LiNi_{0.895}Co_{0.08}Al_{0.02}Hf_{0.005}O_2$	30	2.7–4.3	221/219 (0.1 C)	82/95.3 (100 cycles, 1 C)	[104]
Nb	$LiNi_{0.8}Co_{0.1}Mn_{0.1}O_2$/$Li(Ni_{0.8}Co_{0.1}Mn_{0.1})_{0.999}Nb_{0.001}O_2$	RT	3.0–4.3	186.3/199.9 (0.1 C)	84.12/88.9 (100 cycles, 1 C)	[117]
Ta	$LiNi_{0.939}Co_{0.04}Mn_{0.021}O_2$/$LiNi_{0.935}Co_{0.04}Mn_{0.02}Ta_{0.005}O_2$	30	2.7–4.3	242.1/241.7 (0.1 C)	82/94.8 (100 cycles, 0.5 C)	[118]
V	$LiNi_{0.88}Co_{0.09}Al_{0.03}O_2$/$Li(Ni_{0.88}Co_{0.09}Al_{0.03})_{0.985}V_{0.015}O_2$	25	2.8–4.3	220.1/212.6 (0.1 C)	58.6/84.3 (250 cycles, 2 C)	[107]
W	$LiNi_{0.92}Co_{0.06}Al_{0.02}O_2$/$Li(Ni_{0.92}Co_{0.06}Al_{0.02})_{0.99}W_{0.01}O_2$	25	2.8–4.3	221.6/216.6 (0.2 C)	53/85.6 (100 cycles, 1 C)	[108]
Mo	$Li(Ni_{0.95}Co_{0.03}Mn_{0.02})_{0.99}Al_{0.01}O_2$/$Li(Ni_{0.95}Co_{0.03}Mn_{0.02})_{0.975}Al_{0.01}Mo_{0.015}O_2$	30	2.7–4.3	238.3/236.8 (0.1 C)	87/93.1 (100 cycles, 0.5 C)	[119]

Note: RT represents room temperature.

4. Multicomponent (high-entropy) layered oxides

The so-called high-entropy approach (sometimes also referred to as multicomponent compositionally complex) is considered as a novel and highly promising strategy to improve the electrochemical performance of layered oxide cathodes, including Ni-rich oxides [120– 121]. All multicomponent cathode materials that will be discussed in this section are listed in Table 2, together with the summary of their electrochemical performance and the synthesis route used. As shown in Table 2, these materials can be obtained by various synthesis methods and, despite the presence of multiple different components, all cited studies indicate that there are no significant issues with reaching the desired homogeneity. Before presenting the current state of knowledge and its advantages strictly for Ni-rich cathodes (see below), the original high-entropy concept can be presented for other layered cathode materials. For example, in the search for synergistic effects originating from the presence of several different ele-

Table 2. Summary of the recent studies on multicomponent (high-entropy) cathode materials for Li-ion cells

Strategy	Composition	Synthesis route	Initial discharge capacity / ($mAh \cdot g^{-1}$)	Capacity retention / %	Ref.
Near-equimolar approach	$LiNi_{0.2}Co_{0.2}Mn_{0.2}Al_{0.2}Zn_{0.2}O_2$	NSP	58 (0.1 C, 3–4.5 V)	38 (20 cycles, 0.1 C, 3–4.5 V)	[122]
	$LiNi_{0.2}Co_{0.2}Mn_{0.2}Al_{0.2}Fe_{0.2}O_2$	NSP	43 (0.1 C, 3–4.5 V)	9 (20 cycles, 0.1 C, 3–4.5 V)	[122]
	$Li_{0.8}Na_{0.2}Ni_{0.2}Co_{0.2}Mn_{0.2}Al_{0.2}Fe_{0.2}O_2$	NSP	99 (0.1 C, 3–4.5 V)	68 (20 cycles, 0.1 C, 3–4.5 V)	[122]
	$LiNi_{0.2}Mn_{0.2}Co_{0.2}Fe_{0.2}Ti_{0.2}O_2$	Modified Pechini	160 (0.05 C, 2.5–4.4 V)	53 (50 cycles, 0.1 C, 2.5–4.4 V)	[123]
	$LiCr_{0.167}Mn_{0.167}Fe_{0.167}Co_{0.167}Ni_{0.167}Cu_{0.167}O_2$	PLD (epitaxial thin film)	Not studied	Not studied	[124]
	$LiNi_{0.25}Mn_{0.25}Co_{0.25}Cr_{0.25}O_2$	SCS	162 (20 $mA \cdot g^{-1}$, 2–4.8 V)	46 (50 cycles, 20 $mA \cdot g^{-1}$, 2–4.8 V)	[125]
	$LiNi_{0.2}Mn_{0.2}Co_{0.2}Cr_{0.2}Fe_{0.2}O_2$	SCS	145 (20 $mA \cdot g^{-1}$, 2–4.8 V)	34 (50 cycles, 20 $mA \cdot g^{-1}$, 2–4.8 V)	[125]
Multicomponent doping approach	$LiNi_{0.8}Mn_{0.13}Ti_{0.02}Mg_{0.02}Nb_{0.01}Mo_{0.02}O_2$	Co-precipitation	210 (0.1 C, 2.5–4.4 V)	98 (100 cycles, 1/3 C, 2.5–4.5 V)	[120]
	$Li_{1.15}Mn_{0.5}Ni_{0.15}Co_{0.1}Fe_{0.025}Cu_{0.025}Al_{0.025}Mg_{0.025}O_2$	Sol–gel	284 (0.1 C, 2.1–4.8 V)	93 (100 cycles, 0.1 C, 2.1–4.8 V)	[126]
High-entropy DRX	$Li_{1.3}Mn_{0.2}Co_{0.1}Cr_{0.1}Ti_{0.1}Nb_{0.2}O_{1.7}F_{0.3}$	Solid-state	307 (20 $mA \cdot g^{-1}$, 1.5–4.7 V)	74 (20 $mA \cdot g^{-1}$, 1.5–4.7 V)	[127]
	$Li_{1.25}Ni_{0.1}Co_{0.1}Fe_{0.1}Cr_{0.1}Ti_{0.2}Nb_{0.15}O_{1.8}F_{0.2}$	Solid-state	278 (20 $mA \cdot g^{-1}$, 1.5–4.8 V)	87 (30 cycles, 20 $mA \cdot g^{-1}$, 1.5–4.8 V)	[128]

Note: NSP—Nebulized spray pyrolysis; PLD—Pulsed laser deposition; SCS—Solution combustion synthesis; DRX—Disordered rocksalt oxides/oxyfluorides with Li-excess.

ments in (near) equimolar ratio and high configurational entropy, Wang *et al.* [122] attempted the first synthesis of Li-containing layered high-entropy oxides. The authors successfully incorporated various cations into the $R\bar{3}m$-type structure, obtaining several new materials, both equimolar and non-equimolar, with a general formula Li_x(M1, M2, …, M*n*)O_2, where M: Ni, Co, Mn, Al, Fe, Zn, Cr, Ti, Zr, Cu. However, all of the tested compounds exhibited rather poor electrochemical performance, likely being a result of the extensive Li/Ni mixing and the presence of redox-inactive cations. The authors selected three compositions for more detailed electrochemical characterization, namely $LiNi_{0.2}Co_{0.2}Mn_{0.2}Al_{0.2}Zn_{0.2}O_2$, $LiNi_{0.2}Co_{0.2}Mn_{0.2}Al_{0.2}Fe_{0.2}O_2$, and $Li_{0.8}Na_{0.2}Ni_{0.2}Co_{0.2}Mn_{0.2}Al_{0.2}Fe_{0.2}O_2$ (details in Table 2). It was found that small changes in the composition significantly influence electrochemical properties. In particular, compared to NCM111, $LiNi_{0.2}Co_{0.2}Mn_{0.2}Al_{0.2}Zn_{0.2}O_2$ exhibited higher reaction voltage, further increased by the substitution of Zn by Fe. Interestingly, the partial replacement of Li by Na (20at%) substantially improved the specific capacity and reversibility. While the exact origins of the observed behavior remain unclear, the authors speculated that it may be related to the larger ionic radius of Na^+ (in reference to Li^+) and/or, in some way, to the increased configurational entropy. In the next study, Sturman *et al.* [123] utilized NCM111 as a benchmark for finding optimal cations through machine learning to produce new high-entropy layered materials. While new single-phase compounds could be successfully obtained, the most promising cathode, $LiNi_{0.2}Mn_{0.2}Co_{0.2}Fe_{0.2}Ti_{0.2}O_2$, exhibited worse capacity retention than conventional counterparts (stable capacity of *ca.* 85 $mAh \cdot g^{-1}$ after 50 cycles at 0.1 C current, cycled in a 2.5–4.4 V range). Another equimolar layered oxide, $LiCr_{0.167}Mn_{0.167}Fe_{0.167}Co_{0.167}Ni_{0.167}Cu_{0.167}O_2$, was produced in the form of an epitaxial thin film [124]. The authors presented a stable operation of the material in a thin-film solid-state cell, although thorough electrochemical studies were not performed. To evaluate the impact of high-entropy on the designed layered cathodes, Kawaguchi *et al.* [125] conducted a detailed systematic investigation of $LiNi_{0.25}Mn_{0.25}Co_{0.25}Cr_{0.25}O_2$ and $LiNi_{0.2}Mn_{0.2}Co_{0.2}Cr_{0.2}Fe_{0.2}O_2$. The in-depth structural and electrochemical analyses revealed that there are two main factors responsible for the inferior performance of the studied compounds in reference to NCM111: (1) cation migration during cycling and mixing between Li in consequence and (2) trapping of cations in tetrahedral sites, both causing local repulsion in the Li layer and blocking the intercalation into adjacent sites. This degradation mechanism, summarized in Fig. 7(a), is characteristic for Cr- and Fe-containing conventional systems. Therefore, the possible benefits from high configurational entropy in the equimolar Li-based layered oxides, even if present, cannot mitigate the drawbacks stemming from the individual properties of a given cation. This is further evidenced by the deteriorated electrochemical performance of $LiNi_{0.2}Mn_{0.2}Co_{0.2}Cr_{0.2}Fe_{0.2}O_2$ in reference to $LiNi_{0.25}Mn_{0.25}Co_{0.25}Cr_{0.25}O_2$ (see Table 2), ascribed to the presence of prone to migration Fe and a decreased amount of the electrochemically-active cations. To summarize, in all presented cases, introduction of a high concentration of elements other than the well-established and optimal Co, Ni, and Mn mixture led to the cation mixing with Li, and the overall performance degradation.

Markedly different results could be obtained by employing multicomponent doping, instead of making layered materials (near) equimolar (Table 2). Excellent evidence of the benefits of such a strategy was documented by Song *et al.* [126], who studied another class of Co-free cathodes, layered Li-rich Mn-based oxides (LMR). Remarkably, introducing only a small total amount of dopants by switching from the

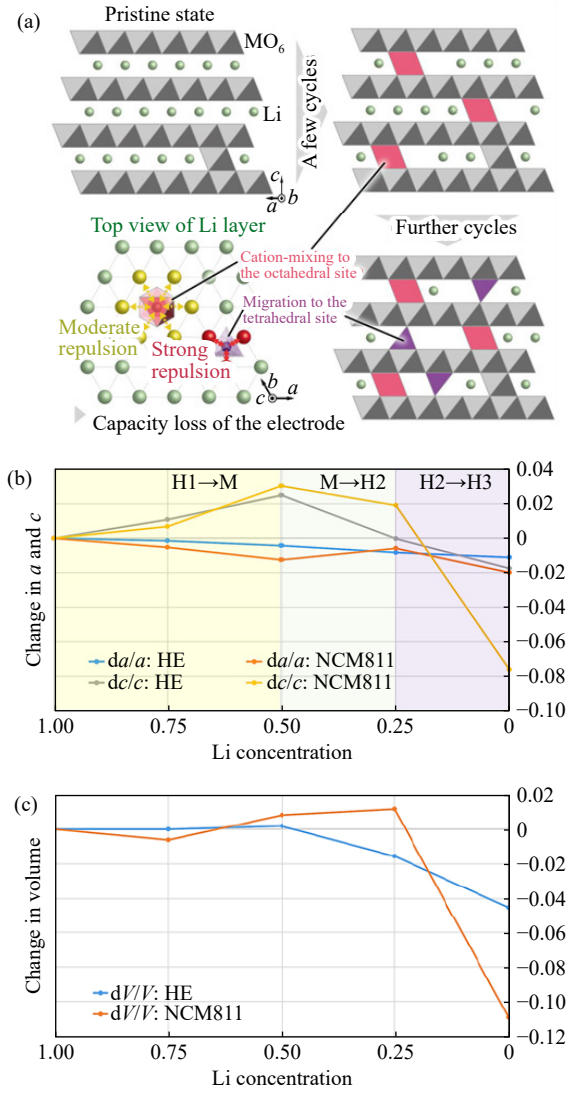

Fig. 7. (a) Illustration of the degradation mechanism for equimolar multicomponent layered cathode materials, $LiNi_{0.25}Mn_{0.25}Co_{0.25}Cr_{0.25}O_2$ and $LiNi_{0.2}Mn_{0.2}Co_{0.2}Cr_{0.2}Fe_{0.2}O_2$, that includes interlayer cation mixing and accumulation of cations in tetrahedral positions, both leading to the capacity loss [125]. Comparison of the change in (b) *a* and *c* lattice parameters and (c) the unit cell volume normalized to the initial values as a function of Li concentration for NMC811 and HE-LNMO with regions related to different phase transitions marked, calculated using density functional theory (DFT). HE-LNMO undergoes much less structural variations [132]. (a) Reprinted with permission from T. Kawaguchi, X. Bian, T. Hatakeyama, H.Y. Li, and T. Ichitsubo, *ACS Appl. Energy Mater.*, vol. 5, 4369-4381 (2022) [125]. Copyright 2022 American Chemical Society. (b, c) Reprinted with permission from A. Bano, M. Noked, and D.T. Major, *Chem. Mater.*, vol. 35, 8426-8439 (2023) [132]. Copyright 2023 American Chemical Society.

typical $Li_{1.2}Mn_{0.54}Ni_{0.13}Co_{0.13}O_2$ (T-LMR) to $Li_{1.15}Mn_{0.5}Ni_{0.15}Co_{0.1}Fe_{0.025}Cu_{0.025}Al_{0.025}Mg_{0.025}O_2$ (HE-LMR), the capacity retention and the stability of voltage profiles, both being the most substantial issues identified for LMR cathodes, were significantly improved (*ca.* 850 $Wh{\cdot}kg^{-1}$ after 100 cycles at 0.1 C between 2.1–4.8 V for HE-LMR compared to *ca.* 425 $Wh{\cdot}kg^{-1}$ for T-LMR). The enhanced performance was ascribed to the increased local (intralayer) structural diversity and lattice distortion, both related to the presence of multiple elements. These features suppressed the activation of low-voltage redox couples, as well as the local (i.a., unwanted interlayer mixing) and global (unfavorable layered to spinel transformation) structural evolution.

Interestingly, the multicomponent compositionally complex (high-entropy) doping approach turned out to be effective also when applied to Ni-rich cathode materials (Table 2). Using the conventional co-precipitation method, Zhang *et al.* [120] synthesized Co-free $LiNi_{0.8}Mn_{0.13}Ti_{0.02}Mg_{0.02}Nb_{0.01}Mo_{0.02}O_2$ (denoted as HE-LNMO) and conducted a comparative study with the state-of-the-art high-Ni NMC811 cathode. The initial discharge specific capacity delivered by HE-LNMO was 210 $mAh{\cdot}g^{-1}$ (voltage range of 2.5–4.4 V), which is comparable to NMC811 (208 $mAh{\cdot}g^{-1}$). However, the initial Coulombic efficiency was improved in the multicomponent material. Interestingly, the polarization difference during the reversible H1 to M (monoclinic) phase transformation was found to be smaller for HE-LNMO and the unfavorable H2–H3 transition was substantially suppressed. Remarkably, the capacity retention tested in the half-cell configuration was much better for HE-LNMO, reaching 98.0% after 50 cycles at 1/3 C (2.5–4.5 V), compared to 85.8% for NMC811. Equally good cycling stability could be achieved in full Li-ion cells, even at a high current of 1 C. In general, the reason for the poor long-term stability of Ni-rich materials is that they undergo very large volume changes during charge/discharge cycles, which causes strain-induced particle cracking, as detected for NMC811. The degradation can be further intensified by irreversible oxygen release at high voltages. For HE-LNMO, those phenomena were significantly suppressed, which resulted in a lack of cracks inside the secondary particles formed during the cell's operation. The volume changes upon cycling (up to 4.3 V) were found to be only 0.3% for HE-LNMO, which is far below NMC811 (5.5%). The authors ascribed this to the pinning effect stemming from multicomponent doping [120]. These undoubtedly very promising results call for the further identification of the phenomena responsible for the improved electrochemical properties of the multicomponent-doped layered cathodes, which are not understood well at the current development stage.

(1) Zero-strain cathode materials.

The materials with volume change below 1.0% are often classified as "zero-strain materials" [129–130]. Pursuing such cathodes is of high importance and has recently been given particular attention in the field [129–131]. The microcracks formed due to volume changes expose fresh surfaces to the electrolyte, which leads to capacity degradation. In extreme cases, the volume expansion/contraction can damage the separator and cause thermal runaway [130]. The utilization of zero-strain materials is even more crucial for the future development of all-solid-state-batteries, as in that case even small volume changes can deteriorate the cathode/electrolyte interface, destroy the coating, or change the pressure

inside a cell [130–131]. In addition to all the advantages of the zero-strain HE-LNMO documented by Zhang *et al.* [120], the material also exhibited excellent thermal stability, substantially better than for other materials containing as much as 0.8 mol of Ni. Importantly, the authors proved the generality of the approach by successfully applying it to other Ni-rich oxides, reaching equally good results. Introducing the new class of high-entropy doped Ni-rich cathodes allowed for the first time mitigating structural degradation and reaching the zero-strain operation without sacrificing the energy density of Ni-rich layered cathodes. In the follow-up study, Bano *et al.* [132] conducted a study using advanced computational analyses in order to elucidate the phenomena responsible for the superior performance of HE-LNMO. Fig. 7(b) and (c) shows the significantly mitigated lattice parameter and volume variation of HE-LNMO compared to NMC811, especially at high delithiation levels. The authors listed five main factors: (1) low crystal lattice variation (multicomponent doping suppresses the lattice deformations); (2) invariant local crystal field environment (consistent environment for oxygen leads to a stable structure); (3) strong metal–oxygen bonding (oxygen pinning blocks the formation of cracks); (4) low degree of anti-site defects (uniform distribution of cations reduces the possibility of the formation of such defects); (5) low operational voltage (more capacity can be delivered without going to high voltages, which prevents oxygen evolution and electrolyte degradation).

Overall, it appears that the original (near) equimolar high-entropy approach is not suitable for designing high-energy-density layered cathodes, as it dilutes the concentration of desirable cations. Contrarily, the multicomponent compositionally complex doping strategy can be effectively implemented, yielding so far unprecedented electrochemical properties for Ni-rich cathodes. It is important to note, however, that at the present stage of the development of multicomponent cathode materials, there is only a limited amount of studies available, which in most cases are focused on introducing new cathode materials rather than on the detailed explanation of how exactly different elements and/or high configurational entropy impact electrochemical performance. Therefore, we call for more studies devoted to the discussion on the relationship between the chemical composition, the value of configuration entropy, and electrochemical properties (e.g., on how the variation of the ratio between cations in a multicomponent system impacts energy density, cyclability, structural stability, etc.).

(2) Disordered rocksalts with Li-excess.

Regarding zero-strain operation, another group of Co-free high-energy-density cathode materials should be also mentioned. Those compounds are disordered rocksalt oxides/oxyfluorides with Li-excess (DRXs) [133–134]. In stark contrast to ordered layered oxides, where even a limited mixing of Li and other cations significantly deteriorates electrochemical performance, the disorder is necessary for efficient Li^+ transport in DRXs. The DRX structure can be considered as a layered structure with 50at% of Li in Li layers randomly replaced by other cations. A sufficient Li-excess combined with extensive cation disorder creates a percolating network for Li^+ through the so-called 0-TM channels. In such a network, Li migration through intermediate tetrahedra occurs in the absence of face-sharing transition metals, enabling facile diffusion with low Coulombic repulsion [133–134]. Numerous DRXs have been reported to exhibit zero-strain operation [130–131,135–136], because they exhibit most of the features defined as necessary for very low volume changes upon cycling [129–130]. To give some examples, Lee *et al.*, who synthesized the first-ever DRX, $Li_{1.211}Mo_{0.467}Cr_{0.3}O_2$, showed that this material undergoes only 0.12% volume change upon charging to 4.3 V [136]. The groups of Yabuuchi *et al.* [131,137–138], Yang *et al.* [135], and Ceder *et al.* [130] demonstrated a few different V-based zero-strain DRX cathode materials. It is worth noting that the high-entropy approach, which promotes disordering unwanted for ordered layered cathodes, can significantly improve the electrochemical performance of DRXs by decreasing unfavorable short-range order. In a comparative study, Lun *et al.* [127] showed that going toward high-entropy DRX oxyfluorides significantly improves the accessible amount of Li and, therefore, the energy density. A similar approach was also proven to be effective for Ni-containing DRXs, as reported by Zhou *et al.* [128]. The summary of the electrochemical performance of selected high-entropy DRX cathodes (enabling the direct comparison with multicomponent ordered layered oxides) is presented in Table 2. To conclude, because of the different structure and diffusion pathways in DRX cathodes compared to layered cathodes, the (near) equimolar high-entropy strategy is a better choice over multicomponent doping to obtain high-energy-density cathodes with zero-strain operation.

5. Coating and surface modification

It is known that interfacial side reactions occurring between the Ni-rich materials and the electrolyte stand out as a primary cause of capacity fading and safety concerns. This is particularly problematic for compounds exhibiting a larger amount of the high-valence Ni^{4+} on the surface (at the charged state). Applying a surface coating on the secondary particles has proven to be an effective strategy to mitigate those side reactions. This includes addressing issues such as electrolyte decomposition and the dissolution of transition metal elements [139–140]. Another problem arises from the presence of LiOH and/or Li_2CO_3 residual lithium sources, originating from a synthesis process. Their occurrence may cause an increase in the pH value of the prepared electrode slurry, causing defluorination of polyvinylidene fluoride (PVDF), cross-linking, and gelation [141–142]. It is especially problematic for the large-scale production of Ni-rich electrodes. Also, side reactions may take place between those compounds and the electrolyte during the cell's operation or storage at high temperatures, resulting in CO, CO_2, and O_2 evolution, causing heat release and serious safety issues [68].

Again, advanced coating may solve this issue, especially if the modifier reacts with lithium residuals [100].

Different approaches have been proposed regarding the coating of Ni-rich materials, with a variety of compounds used including: Al_2O_3 [143], MgO [144], SiO_2 [145], ZnO [146] and TiO_2 [147] oxides, $Co_3(PO_4)_2$/$AlPO_4$ [148], and $Ni_3(PO_4)_2$ [149] phosphates, as well as FeF_3 [150] and AlF_3 [151] fluorides. For example, it was documented by Ryu *et al.* that $Co_3(PO_4)_2$ can react with surface impurities on $LiNi_{0.8}Co_{0.16}Al_{0.04}O_2$, so there is no lithium carbonate present after sintering [152]. However, if the formed coating exhibits low conductivity, the rate performance of the electrode can be affected. On the other hand, it is also possible to construct coatings with good lithium conductivity, including Li_3PO_4 [153–154], Li_2SiO_3 [155], or $Li_2O{\cdot}2B_2O_3$ [156]. Furthermore, different compounds like NH_4VO_3, H_3PO_4, $(NH_4)_2HPO_4$, $ZrO(NO_3)_2{\cdot}4H_2O$, or $NH_4[NbO(C_2O_4)_2(H_2O)_2]{\cdot}3H_2O$ can react with lithium residuals forming ionically-conducting phases [157–160]. Apart from specific works, interested reader can find a broad review about surface coatings of different cathodes for LIBs in the paper by Kaur and Gates [161]. Hereby, only selected, recent results are presented in more detail.

Qu *et al.* [162] developed an integrated surface coating/doping strategy aimed at significantly enhancing the structural stability and electrochemical performance of $LiNi_{0.88}Co_{0.06}Mn_{0.06}O_2$. In this approach, titanium ions derived from a thin $TiNb_2O_7$ coating layer infiltrated the material during the high-temperature sintering process, resulting in the formation of a uniform protective layer on the surface of the secondary particles (Fig. 8(a)). Consequently, side reactions could be effectively suppressed, whereas Ti-doping in-

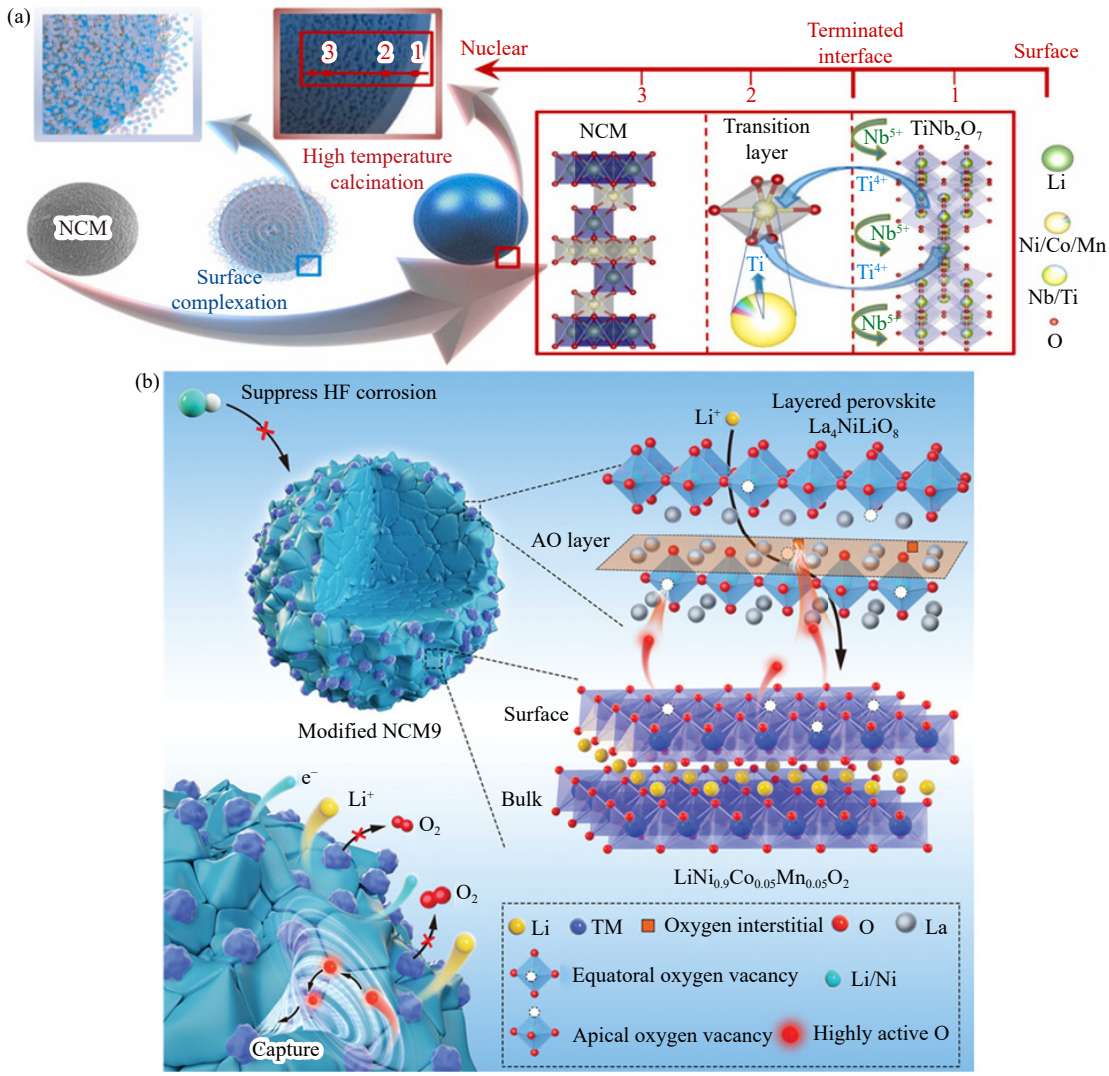

Fig. 8. (a) Diagram of the synthesis process of the modified Ni-rich NCM composites [162]. (b) Schematic diagram of effectively inhibiting the release of highly active oxygenates in the surficial lattice by oxygen vacancies and oxygen interstitials in the layered perovskite La_4NiLiO_8 to improve battery safety performance and alleviate stability issues of ultrahigh-Ni layered oxide cathode materials $LiNi_{0.9}Co_{0.05}Mn_{0.05}O_2$ (NCM9) (AO: rocksalt layer) [163]. (a) Reprinted from *Nano Energy*, Vol. 91, X.Y. Qu, H. Huang, T. Wan, *et al.*, An integrated surface coating strategy to enhance the electrochemical performance of nickel-rich layered cathodes, 106665, Copyright 2022, with permission from Elsevier. (b) L.F. Wang, G.C. Liu, R. Wang, *et al.*, *Adv. Mater.*, vol. 35, 2209483 (2023) [163]. Copyright Wiley-VCH Verlag GmbH & Co. KGaA. Reproduced with permission.

creased the thickness of the lithium layer, and reduced Li/Ni mixing, improving the diffusion of Li^+ in the bulk electrode. The modified material exhibited a remarkable capacity retention of 87.2% after 200 cycles at 1 C, a significant improvement over 59.8% observed in the pristine material. Additionally, first-principles calculations validated the interaction affinity of the $TiNb_2O_7$ coating with the layered $LiNi_{0.88}Co_{0.06}Mn_{0.06}O_2$. Additional achieved benefits were the increased oxygen release energy and enhanced electronic conductivity.

In another paper, Wang *et al.* [163] have introduced a direct regulation strategy to effectively accommodate the highly-active anionic redox within the solid phase. This approach utilizes an advanced coating layer made of a lithium and oxygen dual-ion conductor, layered La_4NiLiO_8 perovskite. This coating layer significantly restrained the reactivity of the (near) surface lattice oxygen, suppressing its release from the lattice, and mitigated the undesired irreversible phase transitions and intergranular mechanical cracking. At the same time, it also facilitated Li^+ diffusion kinetics and enhanced electronic conductivity on the particles surface (Fig. 8(b)). The modified electrode NCM9-LNLO3 exhibited stable cycling over 100 cycles, maintaining a capacity retention of 88.07%. Furthermore, even at a high rate of 10 C, the electrode displayed a notably higher discharge specific capacity of 141.6 $mAh \cdot g^{-1}$, in contrast to the original electrode (87.9 $mAh \cdot g^{-1}$).

Interestingly, Sheng *et al.* [164] designed a stable high-nickel cathode by creating a dense amorphous Li_2CO_3 layer on the particles surface through preemptive atmosphere control. In this case, Li_2CO_3, being the most thermodynamically stable among residual lithium compounds, acts as a physical protective layer, effectively isolating the cathode from exposure to moist air. Additionally, amorphous Li_2CO_3 undergoes transformation into a robust fluorine-rich cathode electrolyte interphase during cycling, reinforcing the cathode's interfacial stability and enhancing electrochemical performance. A high discharge capacity of 232.4 $mAh \cdot g^{-1}$ could be achieved (0.1 C), accompanied by a superior initial Coulombic efficiency of 95.1% and the excellent capacity retention of 90.4% after 100 cycles. Notably, there was no occurrence of slurry gelation during the large-scale electrode fabrication process.

The so-called universal multi-electron surface engineering strategy has been developed by Shen *et al.* to mitigate the instability problems of Ni-rich materials [165]. In this case, Gd_2O_3 was selected to enhance the lithium storage properties of $LiNi_{0.6}Co_{0.05}Mn_{0.35}O_2$. On the one hand, the Gd_2O_3 coating was found to tune the H1–H2 phase transition from a two-phase to a quasi-single-phase reaction, and weakened the harmful H3 phase transition. On the other hand, it also increased the activation energy of the surface lattice oxygen loss, and delayed the phase transition temperature, inhibiting the oxidative decomposition of the electrolyte and harmful interface phase transitions. Thanks to those benefits, the Gd_2O_3-coated NCM showed a weaker discharge median voltage decay after 100 cycles, and the 88.1% capacity retention could be achieved after 400 cycles (1 C).

Also, Zheng *et al.* [166] introduced a straightforward and cost-effective interfacial precipitation–conversion reaction strategy. Employing the high-nickel layered cathode, $LiNi_{0.8}Co_{0.15}Al_{0.05}O_2$, the Zr species were chemically induced on the surface via strong M–PO_4–Zr interactions (M: Ni, Co). After calcination, an ultrathin Zr-containing gradient layer was assembled *in situ*, forming NCA@ZP (Fig. 9). The resulting material demonstrated a high capacity of 219.7 $mAh \cdot g^{-1}$, which is 23% higher than that of the unmodified NCA (179.0 $mAh \cdot g^{-1}$) at 0.1 C. Moreover, it exhibited a superior rate capability, achieving a capacity of 128.2 $mAh \cdot g^{-1}$ at 16 C.

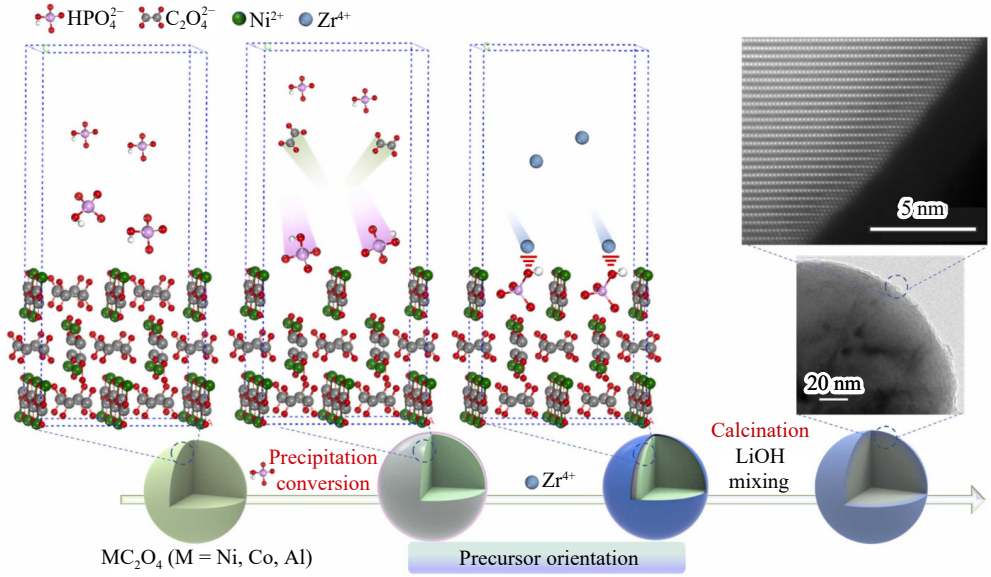

Fig. 9. Schematic illustration of the proposed formation mechanism of the NCA@ZP [166]. Reprinted from *Nano Energy*, Vol. 105, X.Y. Zheng, R.H. Yu, J. Sun, *et al.*, Precursor-oriented ultrathin Zr-based gradient coating on Ni-riched cathodes, 108000, Copyright 2023, with permission from Elsevier.

A summary about different coating types of the high nickel content materials, together with their advantages is presented in Table 3.

6. Single crystal Ni-rich cathode materials

As already discussed, with an increase in Ni content, higher energy density can be achieved in electrodes based on the Ni-rich oxides. However, this enhancement is counterbalanced by (among others) more pronounced interfacial reactions with the electrolyte and worsened safety performance. Single crystal cathode materials offer advantages such as fewer grain boundaries, higher density, and a significant reduction in microcracks during cycling. Consequently, those advantages may help mitigate interfacial side reactions and contribute to improved volumetric energy density and safety [170].

Huang *et al.* [171] introduced a method known as pulse high-temperature sintering (PHTS) for the synthesis of single crystal $LiNi_{0.9}Co_{0.05}Mn_{0.05}O_2$ (SC-NCM90). This approach involved an additional PHTS step at 1040°C for 1 min alongside the conventional calcination process conducted at 750°C. Well-defined octahedral particles could be formed, showing an initial capacity of 209 $mAh \cdot g^{-1}$ (0.05 C). In comparison to NCM90 secondary spheres, SC-NCM90 exhibited a 1/3 increase in tap density, reaching 2.76 $g \cdot cm^{-3}$. The formation of microcracks was effectively suppressed during cycling. The authors also provided in their work simulated crystal growth data, as presented in Fig. 10.

Ran *et al.* [172] conducted a study on both polycrystalline (P-NCM811) and single crystal (S-NCM811) cathode materials to investigate the impact of aging mechanisms in nanocrystalline grains on electrochemical performance. The findings revealed that the capacity retention of the S-NCM811 cathode gradually decreases to 80% after 200 cycles at a 1 C rate, while for the P-NCM811 it was 72%. In-depth analyses using *in situ* X-ray diffraction and *ex situ* scanning electron microscopy suggested that irreversible structural and phase transformations significantly affected the performance of the polycrystalline material. The research also indicated that surface side reactions and structural defects resulting from internal crystal domains can impede the diffusion of Li^+, leading to rapid capacity fading.

In another paper, Hu *et al.* [173] took $LiNi_{0.76}Mn_{0.14}Co_{0.1}O_2$ (NMC76) as a model material to study the mechanism of gas generation from single crystal and polycrystalline NMC. Even at elevated potentials, the amount of gases detected from the single crystal sample was much lower than those from the polycrystalline one, indicating that the drastically reduced number of boundaries and surface area in the single crystal sample suppressed surface side reactions (Fig. 11). It was also found that oxygen was accumulated in the polycrystalline NMC76, observable in full pouch cells tested at relevant conditions.

Other authors noted that the inadequate thermal stability of polycrystalline NCM materials has been consistently a conspicuous drawback, and the thermal performance of single crystal materials is also a crucial factor that cannot be overlooked. Kong *et al.* [174] conducted a study using $LiNi_{0.8}Co_{0.1}Mn_{0.1}O_2$ and $LiNi_{0.6}Co_{0.2}Mn_{0.2}O_2$ materials with both single crystal (SC) and polycrystalline (PC) morphology to examine their thermal characteristics (Fig. 12). The results indicated that single crystal materials exhibit significantly better thermal stability, while the presence of internal crystal gaps in polycrystalline materials resulted in a higher Li^+ transport impedance and a lower diffusion coefficient. This led to increased heat generation during the cycling process. Simultaneously, crystal gaps contribute to the inhomogeneity during (dis-)charging, so the structural damage becomes more severe. This can be a triggering factor for dangerous oxygen release.

7. Gradient modification

Functionally graded materials (FGM) are characterized by the changing composition and/or microstructure, distributed with a directional gradient. Gradient distributions can be one-, two-, or three-dimensional. It is important to note that gradient materials should be distinguished from the surface-modified ones (with surface coatings), as in the latter case, two essentially different materials form a clear interface [175]. Taking a gradient Ni-rich cathode oxide as an example, in which the concentration of transition metals varies continuously from the bulk to surface, it can be expected that the lattice parameter mismatch at the core and shell interface can be minimized. This should help preventing formation of the

Table 3. Summary of coating types of the Ni-rich materials and their advantages

Type of coatings	Coating materials	Main advantages	Ref.
Oxide coatings	Al_2O_3, MgO, SiO_2, ZnO, TiO_2	Improve interface stability; clear HF to alleviate cation dissolution (SiO_2)	[144,167]
Phosphate coatings	$Co_3(PO_4)_2$, $AlPO_4$, $Ni_3(PO_4)_2$, $FePO_4$	Enhance the thermal stability polyanions; inhibit oxygen release from the cathode lattices; facilitate lithium diffusion channels	[148–149]
Fluoride coatings	FeF_3, AlF_3	Improve resistance to HF attack; good ionic and electronic conductivity	[150–151]
Lithium composite coatings	Li_3PO_4, Li_2SiO_3, $Li_2O \cdot 2B_2O_3$	Improve lithium-ion mobility and improve rate performance	[153–154]
Carbon coatings	Carbon, graphene oxide, reduced graphene oxide (RGO), graphite	Provide high electronic conductivity	[168]
Other coatings	Polymers, lithium rich materials, metals	Improve interface stability; reduce the amount of residual lithium	[169]

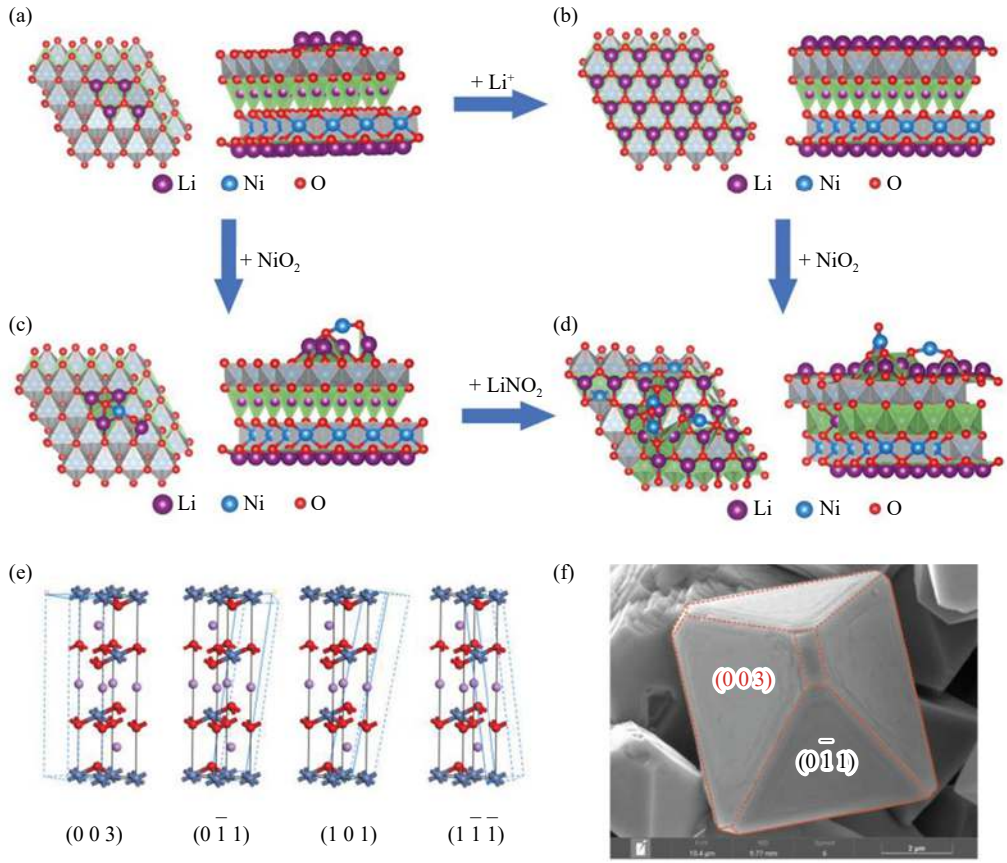

Fig. 10. (a–d) Simulated crystal growth layer by layer starting from the state of four Li ions deposited on $LiNiO_2$ (001) substrate. Here, transition metal elements are represented by Ni as a simplified model. (e) Cleaving methods of NCM811 crystal for facets (003), (0$\bar{1}$1), (101), and (1$\bar{1}\bar{1}$). The solid blue wireframes are the locations of the crystal planes to be cleaved and the dotted blue wireframes are the extension of the slabs to be constructed. (f) A SC-NCM811 particle with crystal facet indexes on the surface. H. Huang, L.P. Zhang, H.Y. Tian, *et al.*, *Adv. Energy Mater.*, vol. 13, 2203188 (2023) [171]. Copyright Wiley-VCH Verlag GmbH & Co. KGaA. Reproduced with permission.

gaps at the core/shell interface after long-term cycling, and thereby improving the cycle stability [176]. However, slight reduction of the reversible capacity may be expected [13].

Advanced modifications of the Ni-rich materials have been already performed using the mentioned concentration gradient approach. For example, Park *et al.* [13] developed $LiNi_{0.865}Co_{0.120}Al_{0.015}O_2$ cathode material, in which a core within each secondary particle maintains a consistent nickel-rich composition to optimize discharge capacity, but the outer layer exhibits a decreasing nickel concentration and increasing cobalt concentration toward the particle surface. This was done to enhance structural and chemical stability. The cobalt-rich surface and gradient structure effectively alleviated the internal strain, bolstering resistance to electrolyte erosion. This design also accommodated anisotropic volume changes during cycling. The developed gradient NCA cathode demonstrated superior performance, delivering a reversible capacity of more than 220 $mAh \cdot g^{-1}$ (0.5 C) and retaining 90% of the initial capacity even after 100 cycles at 60°C.

Notably, Lin *et al.* [177] designed and synthesized $LiNi_{0.8}Mn_{0.1}Co_{0.1}O_2$ that is uniform in composition, but exhibits a nickel valence state gradient along the radial direction of secondary particles (contrary to more common concentration gradient materials). This enhancement led to the improved cycling stability and thermal stability of the material. Notably, after 100 cycles, the valence gradient cathode maintained a specific capacity above 175 $mAh \cdot g^{-1}$ (0.1 C), outperforming the traditional NMC811 tested under the same conditions.

It is worth noting that the current large-scale preparation methods of Ni-rich cathodes include the solid phase method, co-precipitation method, spray drying, sol–gel, and other techniques [178]. Among them, the co-precipitation method is very suitable for synthesizing concentration gradient structural materials, so the gradient modification should not present major obstacles in the large-scale production of Ni-rich cathodes.

8. New electrolytes and their modification

In addition to all modification methods mentioned above, such as coating or doping, that aim to enhance the cycling performance of Ni-rich layered cathodes in LIBs taking an approach from the electrode material perspective, there are also many research activities to develop new electrolytes and/or their functional additives. Those additives have already demonstrated the ability to improve the Coulombic efficiency and cycle life of such cathodes through a simple,

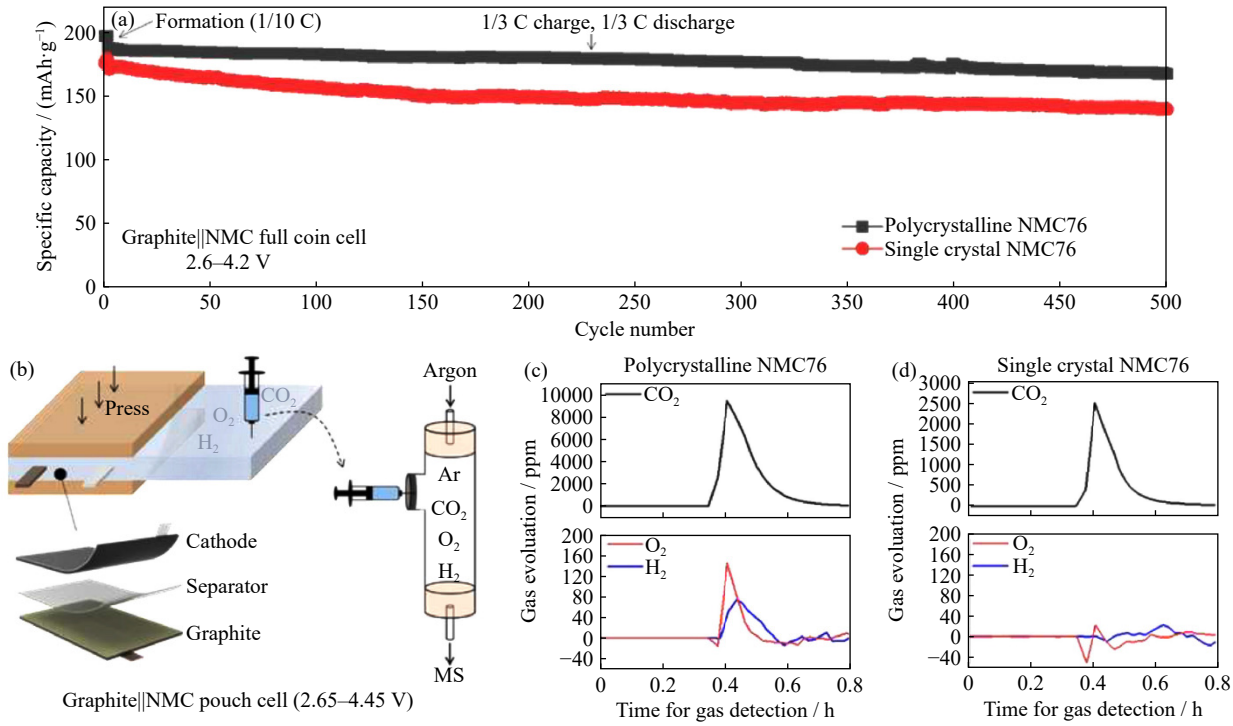

Fig. 11. Gas analysis of polycrystalline and single crystal NMC76 in pouch cells: (a) cycling stability of polycrystalline and single crystal NMC76 with graphite as the counter electrode. The cells are cycled between 2.7 and 4.2 V using graphite as the anode in coin cells. The mass loading of NMC76 is around 12 mg·cm^{-2}. (b) Schemes for single layer pouch cell for gas collection and transfer. Quantified amounts of CO_2, O_2, and H_2 in pouch cells after 200 cycles of (c) polycrystalline NMC76 and (d) single crystal NMC76 [173]. Reprinted from *Energy Storage Mater.*, Vol. 47, J.T. Hu, L.Z. Li, Y.J. Bi, *et al.*, Locking oxygen in lattice: A quantifiable comparison of gas generation in polycrystalline and single crystal Ni-rich cathodes, 195-202, Copyright 2022, with permission from Elsevier.

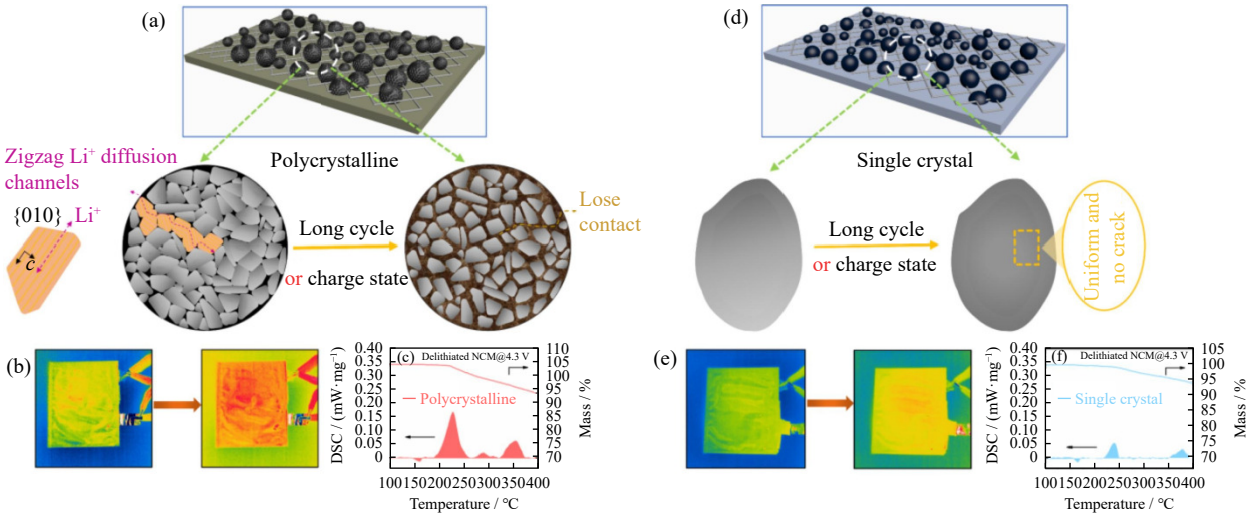

Fig. 12. (a) Schematic diagram of PC materials; (b) temperature rise of a pouch cell composed of PC materials cycling at a high rate; (c) differential scanning calorimetry (DSC) test of delithiated PC materials; (d) schematic diagram of SC materials; (e) temperature rise of a battery composed of SC materials cycling at a high rate; (f) DSC test of delithiated SC materials [174]. Reprinted from *Chem. Eng. J.*, Vol. 434, X.B. Kong, Y.G. Zhang, J.Y. Li, *et al.*, Single-crystal structure helps enhance the thermal performance of Ni-rich layered cathode materials for lithium-ion batteries, 134638, Copyright 2022, with permission from Elsevier.

effective, and economical approach. Specifically, undesired substances, such as HF and H_2O, can be removed and/or a stable protective CEI layer can be formed to mitigate detrimental effects. The uniform, thin, and dense CEI layer can serve multiple purposes [55]: to facilite Li^+ diffusion, reduce interface resistance, prevent transition metal dissolution, and cover active sites prone to catalyzing electrolyte decomposition. Among the compounds of interest, vinylene carbonate (VC) [179], fluoroethylene carbonate (FEC) [180], and tris(2,2,2-trifluoroethyl)phosphite (TTFP) [181] should be mentioned. A full review on this topic was recently published by Li *et al.* [37] (Table 4).

Table 4. A summary of the electrolyte functional additives for cells based on Ni-rich cathodes, together with their mechanism of action. Based on Ref. [37]. For the abbreviations, please see the references or the review [37]

Types of electrolyte additives	Functional additives	Effects and working mechanisms	Ref.
Sulfone groups based functional additives	TOSMIC, PTSS, SDM, BFS, DPS, DVS, PTSI, AS, NTESA, PS, PST, MMDS	Beneficial to form a stable and protective CEI layer in Ni-rich cathodes, due to their high oxidative stability	[182]
Phosphates and phosphites functional additives	EDP, THFPP, TFEOP, PFPOP, HFiPOP, MDPCT, TFPCT, CETPE, TPPO, MDPO, DEPP, TAPi, TEP, TTFP, TMPi, TPP, LiDFBP	Have a flame-retardant effect and participate in the formation of the CEI protective layer on the nickel-rich cathode	[183]
Silicon-based additives	TMSPi, TMSPa, TMSB, LTB, BTMSMFM, DODSi, IPTS, DPDMS, BSA, NNB, DSON, TMS-ON	Resist or remove HF and reduce TM dissolution	[184]
Borate-based additives	TEAB, ABAPE, TIB, TPB, PBF, PRZ, LiBOB, LiDFOB	Generate borate-based CEI, which can effectively inhibit electrolyte decomposition and TM dissolution of Ni	[185]
VC and ester-based additives	VC, DPC, MPC, SA	Form CEI layer on the surface of nickel-rich cathode to improve cycle stability	[186]
Additives containing fluoroalkyl groups	ETFB, FEMC, FEC, DFEAc, TTE	Help to form a stable and dense CEI protective layer, which can effectively reduce intergranular cracking of nickel-rich cathodes	[187]

9. Ni-rich cathodes in solid-state batteries

With the strong interest in development of all solid-state batteries (ASSBs), there are obviously reports on the application of Ni-rich cathodes in such cells, showing promising results, but indicating still unresolved problems with electrochemical performance [188–193]. Among the published papers, the results of Deng *et al.* [194] showed the effectiveness of the bifunctional Li_3PO_4 modification devised for Ni-rich layered oxide cathodes in sulfide-based ASSBs. This modification served two purposes: to mitigate side-reactions with the $Li_{10}GeP_2S_{12}$ sulfide electrolyte and suppress microstructural cracks emerging upon (dis-)charging cycles. Compared to the bare cathode, the modified one exhibited a notably improved initial capacity of 170.6 $mAh \cdot g^{-1}$ at 0.1 C, superior rate performance, and reduced polarization. Furthermore, stable performance was achieved during 300 cycles, with the capacity fade of only 0.22 $mAh \cdot g^{-1}$ per cycle at 0.2 C.

10. Brief conclusions and perspectives

As documented in this paper, there is still a strong interest in the further development of Ni-rich cathode materials, and there are numerous new concepts emerging (i.a., single crystal morphology, multicomponent doping, gradient composition, etc.), based on which intrinsic issues hindering the application of those compounds, can be (at least partially) resolved. Indeed, the state-of-the-art Ni-rich designs already offer the possibility of the construction of high energy-density LIBs, as stability, safety, and long-term operation are already at the acceptable level. Nevertheless, there is always a question about costs, as well as the scalability of the preparation process. In fact, some of the proposed advanced and usually complex approaches are hardly transferable to the commercial scale, while further modification of different proposed solutions may bring cheap and easily scalable technology to the industry. Also, with new Co-free cathode materials and an interest in developing Li-rich alternatives, it is not unimaginable that the next, rather revolutionary, step would possibly be Co- and Ni-free cathodes. Nevertheless, research focusing on materials engineering, electrolytes innovation, and advanced manufacturing processes is the key to overcome the remaining challenges and should help unlock the benefits of the application of Ni-rich cathodes for a wider range of commercial cells.

Acknowledgements

This work was supported by the program "Excellence Initiative - Research University" for the AGH University of Krakow (IDUB AGH, No. 501.696.7996, Action 4, ID 6354). This work was partially supported by the AGH University of Krakow under No. 16.16.210.476.

Conflict of Interest

Konrad Świerczek is the Executive Editor-in-Chief of this journal and was not involved in the editorial review or the decision to publish this article. All authors declare that they have no conflicts of interest.

Open Access Funding provided by the Poland ICM.

References

[1] S.C. Jiao, J.Y. Wang, Y.S. Hu, X.Q. Yu, and H. Li, High-capacity oxide cathode beyond 300 mAh/g, *ACS Energy Lett.*, 8(2023), No. 7, p. 3025.

[2] Y.K. Sun, High-capacity layered cathodes for next-generation electric vehicles, *ACS Energy Lett.*, 4(2019), No. 5, p. 1042.

[3] J.J. Xu, X.Y. Cai, S.M. Cai, *et al.*, High-energy lithium-ion batteries: Recent progress and a promising future in applications, *Energy Environ. Mater.*, 6(2023), No. 5, art. No. e12450.

[4] A. Aishova, G.T. Park, C.S. Yoon, and Y.K. Sun, Cobalt-free high-capacity Ni-rich layered $Li[Ni_{0.9}Mn_{0.1}]O_2$ cathode, *Adv. Energy Mater.*, 10(2020), No. 4, art. No. 1903179.

[5] J.R. Dahn, U.V. Sacken, and C.A. Michal, Structure and electrochemistry of $Li_{1\pm y}NiO_2$ and a new Li_2NiO_2 phase with the $Ni(OH)_2$ structure, *Solid State Ionics*, 44(1990), No. 1-2, p. 87.

[6] H.H. Ryu, N.Y. Park, J.H. Seo, *et al.*, A highly stabilized Ni-rich NCA cathode for high-energy lithium-ion batteries, *Mater. Today*, 36(2020), p. 73.

[7] L.S. Li, Z. Zhang, S.H. Fu, Z.Z. Liu, and Y.M. Liu, Co-modification by $LiAlO_2$-coating and Al-doping for $LiNi_{0.5}Co_{0.2}Mn_{0.3}O_2$ as a high-performance cathode material for lithium-ion batteries with a high cutoff voltage, *J. Alloys Compd.*, 768(2018), p. 582.

[8] T. Ohzuku and Y. Makimura, Layered lithium insertion material of $LiCo_{1/3}Ni_{1/3}Mn_{1/3}O_2$ for lithium-ion batteries, *Chem. Lett.*, 30(2001), No. 7, p. 642.

[9] J.G. Gao, Z.P. Qin, G.Y. Zhao, *et al.*, Modulating NCM622 electrode to efficiently boost the lithium storage and thermal safety of its full batteries, *Energy Storage Mater.*, 67(2024), art. No. 103332.

[10] S.L. Wang, S.M. Chen, W.Q. Gao, L.L. Liu, and S.J. Zhang, A new additive 3-Isocyanatopropyltriethoxysilane to improve electrochemical performance of Li/NCM622 half-cell at high voltage, *J. Power Sources*, 423(2019), p. 90.

[11] Z.S. Wang, C.L. Zhu, J.D. Liu, *et al.*, Catalytically induced robust inorganic-rich cathode electrolyte interphase for 4.5 V Li||NCM622 batteries, *Adv. Funct. Mater.*, 33(2023), No. 19, art. No. 2212150.

[12] G. Salitra, E. Markevich, M. Afri, *et al.*, High-performance cells containing lithium metal anodes, $LiNi_{0.6}Co_{0.2}Mn_{0.2}O_2$ (NCM 622) cathodes, and fluoroethylene carbonate-based electrolyte solution with practical loading, *ACS Appl. Mater. Interfaces*, 10(2018), No. 23, p. 19773.

[13] K.J. Park, M.J. Choi, F. Maglia, *et al.*, High-capacity concentration gradient $Li[Ni_{0.865}Co_{0.120}Al_{0.015}]O_2$ cathode for lithium-ion batteries, *Adv. Energy Mater.*, 8(2018), No. 19, art. No. 1703612.

[14] C.M. Julien and A. Mauger, NCA, NCM811, and the route to Ni-richer lithium-ion batteries, *Energies*, 13(2020), No. 23, art. No. 6363.

[15] F. Reuter, A. Baasner, J. Pampel, *et al.*, Importance of capacity balancing on the electrochemical performance of $Li[Ni_{0.8}Co_{0.1}Mn_{0.1}]O_2$ (NCM811)/silicon full cells, *J. Electrochem. Soc.*, 166(2019), No. 14, p. A3265.

[16] H.L. Zhang and J.J. Zhang, An overview of modification strategies to improve $LiNi_{0.8}Co_{0.1}Mn_{.1}O_2$ (NCM811) cathode performance for automotive lithium-ion batteries, *eTransportation*, 7(2021), art. No. 100105.

[17] L.H. Zhang, F.Q. Min, Y. Luo, *et al.*, Practical 4.4 V Li||NCM811 batteries enabled by a thermal stable and HF free carbonate-based electrolyte, *Nano Energy*, 96(2022), art. No. 107122.

[18] M.Y. Zhang, C.Y. Wang, J.K. Zhang, G. Li, and L. Gu, Preparation and electrochemical characterization of La and Al co-doped NCM811 cathode materials, *ACS Omega*, 6(2021), No. 25, p. 16465.

[19] Y.Z. Zheng, N.B. Xu, S.J. Chen, *et al.*, Construction of a stable $LiNi_{0.8}Co_{0.1}Mn_{0.1}O_2$ (NCM811) cathode interface by a multifunctional organosilicon electrolyte additive, *ACS Appl. Energy Mater.*, 3(2020), No. 3, p. 2837.

[20] W.D. Li, X.M. Liu, Q. Xie, Y. You, M.F. Chi, and A. Manthiram, Long-term cyclability of NCM-811 at high voltages in lithium-ion batteries: An In-depth diagnostic study, *Chem. Mater.*, 32(2020), No. 18, p. 7796.

[21] S.S. Zhang, Understanding of performance degradation of $LiNi_{0.80}Co_{0.10}Mn_{0.10}O_2$ cathode material operating at high potentials, *J. Energy Chem.*, 41(2020), p. 135.

[22] M.H. Kim, H.S. Shin, D. Shin, and Y.K. Sun, Synthesis and electrochemical properties of $Li[Ni_{0.8}Co_{0.1}Mn_{0.1}]O_2$ and $Li[Ni_{0.8}Co_{0.2}]O_2$ via co-precipitation, *J. Power Sources*, 159(2006), No. 2, p. 1328.

[23] Y. Cheng, X.Z. Zhang, Q.Y. Leng, *et al.*, Boosting electrochemical performance of Co-free Ni-rich cathodes by combination of Al and high-valence elements, *Chem. Eng. J.*, 474(2023), art. No. 145869.

[24] W.B. Hua, J.L. Zhang, S.N. Wang, *et al.*, Long-range cationic disordering induces two distinct degradation pathways in Co-free Ni-rich layered cathodes, *Angew. Chem. Int. Ed.*, 62(2023), No. 12, art. No. e202214880.

[25] H. Li, L. Wang, Y.Z. Song, *et al.*, Understanding the insight mechanism of chemical-mechanical degradation of layered Co-free Ni-rich cathode materials: A review, *Small*, 19(2023), No. 32, art. No. 2302208.

[26] N. Li, S. Sallis, J.K. Papp, B.D. McCloskey, W.L. Yang, and W. Tong, Correlating the phase evolution and anionic redox in Co-Free Ni-Rich layered oxide cathodes, *Nano Energy*, 78(2020), art. No. 105365.

[27] A. Liu, N. Zhang, J.E. Stark, P. Arab, H.Y. Li, and J.R. Dahn, Synthesis of Co-free Ni-rich single crystal positive electrode materials for lithium ion batteries: Part I. two-step lithiation method for Al- or Mg-doped $LiNiO_2$, *J. Electrochem. Soc.*, 168(2021), No. 4, art. No. 040531.

[28] J.J. Liu, Y.F. Yuan, J.H. Zheng, *et al.*, Understanding the synthesis kinetics of single-crystal Co-free Ni-rich cathodes, *Angew. Chem. Int. Ed.*, 62(2023), No. 20, art. No. e202302547.

[29] T.C. Liu, L. Yu, J.J. Liu, *et al.*, Understanding Co roles towards developing Co-free Ni-rich cathodes for rechargeable batteries, *Nat. Energy*, 6(2021), No. 3, p. 277.

[30] L.S. Ni, R.T. Guo, S.S. Fang, *et al.*, Crack-free single-crystalline Co-free Ni-rich $LiNi_{0.95}Mn_{0.05}O_2$ layered cathode, *eScience*, 2(2022), No. 1, p. 116.

[31] Y.L. Liu, P.H. Xiao, G.A. Botton, *et al.*, Tungsten infused grain boundaries enabling universal performance enhancement of Co-free Ni-rich cathode materials, *J. Electrochem. Soc.*, 168(2021), No. 12, art. No. 120514.

[32] N. Voronina, Y.K. Sun, and S.T. Myung, Co-free layered cathode materials for high energy density lithium-ion batteries, *ACS Energy Lett.*, 5(2020), No. 6, p. 1814.

[33] C. Wang, L. Tan, H.L. Yi, *et al.*, Unveiling the impact of residual Li conversion and cation ordering on electrochemical performance of Co-free Ni-rich cathodes, *Nano Res.*, 15(2022), No. 10, p. 9038.

[34] Y.K. Xi, M.J. Wang, L. Xu, *et al.*, A new Co-free Ni-rich $LiNi_{0.8}Fe_{0.1}Mn_{0.1}O_2$ cathode for low-cost Li-ion batteries, *ACS Appl. Mater. Interfaces*, 13(2021), No. 48, p. 57341.

[35] J.U. Choi, N. Voronina, Y.K. Sun, and S.T. Myung, Recent progress and perspective of advanced high-energy Co-less Ni-rich cathodes for Li-ion batteries: Yesterday, today, and tomorrow, *Adv. Energy Mater.*, 10(2020), No. 42, art. No. 2002027.

[36] S. Jamil, G. Wang, M. Fasehullah, and M.W. Xu, Challenges and prospects of nickel-rich layered oxide cathode material, *J.*

Alloys Compd., 909(2022), art. No. 164727.
[37] L.S. Li, D.M. Wang, G.J. Xu, *et al*., Recent progress on electrolyte functional additives for protection of nickel-rich layered oxide cathode materials, *J. Energy Chem.*, 65(2022), p. 280.
[38] Y. Lu, Y.D. Zhang, Q. Zhang, F.Y. Cheng, and J. Chen, Recent advances in Ni-rich layered oxide particle materials for lithium-ion batteries, *Particuology*, 53(2020), p. 1.
[39] H.H. Ryu, H.H. Sun, S.T. Myung, C.S. Yoon, and Y.K. Sun, Reducing cobalt from lithium-ion batteries for the electric vehicle era, *Energy Environ. Sci.*, 14(2021), No. 2, p. 844.
[40] C. Xu, P.J. Reeves, Q. Jacquet, and C.P. Grey, Phase behavior during electrochemical cycling of Ni-rich cathode materials for Li-ion batteries, *Adv. Energy Mater.*, 11(2021), No. 7, art. No. 2003404.
[41] S.S. Zhang, Problems and their origins of Ni-rich layered oxide cathode materials, *Energy Storage Mater.*, 24(2020), p. 247.
[42] A. Chakraborty, S. Kunnikuruvan, S. Kumar, *et al*., Layered cathode materials for lithium-ion batteries: Review of computational studies on $LiNi_{1-x-y}Co_xMn_yO_2$ and $LiNi_{1-x-y}Co_xAl_yO_2$, *Chem. Mater.*, 32(2020), No. 3, p. 915.
[43] J. Yang, X.H. Liang, H.H. Ryu, C.S. Yoon, and Y.K. Sun, Ni-rich layered cathodes for lithium-ion batteries: From challenges to the future, *Energy Storage Mater.*, 63(2023), art. No. 102969.
[44] S. Lee, L.S. Su, A. Mesnier, Z.H. Cui, and A. Manthiram, Cracking vs. surface reactivity in high-nickel cathodes for lithium-ion batteries, *Joule*, 7(2023), No. 11, p. 2430.
[45] Z.H. Cui and A. Manthiram, Thermal stability and outgassing behaviors of high-nickel cathodes in lithium-ion batteries, *Angew. Chem. Int. Ed.*, 62(2023), No. 43, art. No. e202307243.
[46] Z.Z. Cui, X. Li, X.Y. Bai, X.D. Ren, and X. Ou, A comprehensive review of foreign-ion doping and recent achievements for nickel-rich cathode materials, *Energy Storage Mater.*, 57(2023), p. 14.
[47] Y. Kim, H. Park, J.H. Warner, and A. Manthiram, Unraveling the intricacies of residual lithium in high-Ni cathodes for lithium-ion batteries, *ACS Energy Lett.*, 6(2021), No. 3, p. 941.
[48] B.Y. Fu, A. Kulka, B. Wang, *et al*., Ni-rich $LiNi_{0.905}Co_{0.043}Al_{0.052}O_2$ cathode material for high-energy density Li-ion cells: Tuning lithium content, structural evolution, and full-cell performance, *Electrochim. Acta*, 494(2024), art. No. 144455.
[49] M. Liu, Y. Jiang, Y.P. Qin, Z.J. Feng, D.Y. Wang, and B.K. Guo, Enhanced electrochemical performance of Ni-rich cathodes by neutralizing residual lithium with acid compounds, *ACS Appl. Mater. Interfaces*, 13(2021), No. 46, p. 55072.
[50] M. Jiang, D.L. Danilov, R.A. Eichel, and P.H.L. Notten, A review of degradation mechanisms and recent achievements for Ni-rich cathode-based Li-ion batteries, *Adv. Energy Mater.*, 11(2021), No. 48, art. No. 2103005.
[51] B. Aktekin, M.J. Lacey, T. Nordh, *et al*., Understanding the capacity loss in $LiNi_{0.5}Mn_{1.5}O_4$–$Li_4Ti_5O_{12}$ lithium-ion cells at ambient and elevated temperatures, *J. Phys. Chem. C*, 122(2018), No. 21, p. 11234.
[52] M. Dixit, B. Markovsky, F. Schipper, D. Aurbach, and D.T. Major, Origin of structural degradation during cycling and low thermal stability of Ni-rich layered transition metal-based electrode materials, *J. Phys. Chem. C*, 121(2017), No. 41, p. 22628.
[53] H.J. Noh, S. Youn, C.S. Yoon, and Y.K. Sun, Comparison of the structural and electrochemical properties of layered $Li[Ni_xCo_yMn_z]O_2$ (x = 1/3, 0.5, 0.6, 0.7, 0.8 and 0.85) cathode material for lithium-ion batteries, *J. Power Sources*, 233(2013), p. 121.
[54] D. Leanza, M. Mirolo, C.A.F. Vaz, P. Novák, and M. El Kazzi, Surface degradation and chemical electrolyte oxidation induced by the oxygen released from layered oxide cathodes in Li-ion batteries, *Batter. Supercaps*, 2(2019), No. 5, p. 482.
[55] J.T. Zhao, Y. Liang, X. Zhang, *et al.*, *In situ* construction of uniform and robust cathode–electrolyte interphase for Li-rich layered oxides, *Adv. Funct. Mater.*, 31(2021), No. 8, art. No. 2009192.
[56] W.M. Dose, I. Temprano, J.P. Allen, *et al*., Electrolyte reactivity at the charged Ni-rich cathode interface and degradation in Li-ion batteries, *ACS Appl. Mater. Interfaces*, 14(2022), No. 11, p. 13206.
[57] R. Jung, M. Metzger, F. Maglia, C. Stinner, and H.A. Gasteiger, Oxygen release and its effect on the cycling stability of $LiNi_xMn_yCo_zO_2$(NMC) cathode materials for Li-ion batteries, *J. Electrochem. Soc.*, 164(2017), No. 7, p. A1361.
[58] S.M. Bak, E.Y. Hu, Y.N. Zhou, *et al*., Structural changes and thermal stability of charged $LiNi_xMn_yCo_zO_2$ cathode materials studied by combined *in situ* time-resolved XRD and mass spectroscopy, *ACS Appl. Mater. Interfaces*, 6(2014), No. 24, p. 22594.
[59] S.K. Jung, H. Gwon, J. Hong,et al., Understanding the degradation mechanisms of $LiNi_{0.5}Co_{0.2}Mn_{0.3}O_2$ cathode material in lithium ion batteries, *Adv. Energy Mater.*, 4(2014), No. 1, art. No. 1300787.
[60] K.W. Nam, S.M. Bak, E.Y. Hu, *et al*., Combining *in situ* synchrotron X-ray diffraction and absorption techniques with transmission electron microscopy to study the origin of thermal instability in overcharged cathode materials for lithium-ion batteries, *Adv. Funct. Mater.*, 23(2013), No. 8, p. 1047.
[61] H. Li, P.F. Zhou, F.M. Liu, H.X. Li, F.Y. Cheng, and J. Chen, Stabilizing nickel-rich layered oxide cathodes by magnesium doping for rechargeable lithium-ion batteries, *Chem. Sci.*, 10(2018), No. 5, p. 1374.
[62] J.H. Kim, H.H. Ryu, S.J. Kim, C.S. Yoon, and Y.K. Sun, Degradation mechanism of highly Ni-rich $Li[Ni_xCo_yMn_{1-x-y}]O_2$ cathodes with $x > 0.9$, *ACS Appl. Mater. Interfaces*, 11(2019), No. 34, p. 30936.
[63] A.O. Kondrakov, A. Schmidt, J. Xu, *et al*., Anisotropic lattice strain and mechanical degradation of high- and low-nickel NCM cathode materials for Li-ion batteries, *J. Phys. Chem. C*, 121(2017), No. 6, p. 3286.
[64] G.W. Nam, N.Y. Park, K.J. Park, *et al*., Capacity fading of Ni-rich NCA cathodes: Effect of microcracking extent, *ACS Energy Lett.*, 4(2019), No. 12, p. 2995.
[65] H.H. Ryu, B. Namkoong, J.H. Kim, I. Belharouak, C.S. Yoon, and Y.K. Sun, Capacity fading mechanisms in Ni-rich single-crystal NCM cathodes, *ACS Energy Lett.*, 6(2021), No. 8, p. 2726.
[66] D.J. Miller, C. Proff, J.G. Wen, D.P. Abraham, and J. Bareño, Observation of microstructural evolution in Li battery cathode oxide particles by *in situ* electron microscopy, *Adv. Energy Mater.*, 3(2013), No. 8, p. 1098.
[67] K.J. Park, J.Y. Hwang, H.H. Ryu, *et al*., Degradation mechanism of Ni-enriched NCA cathode for lithium batteries: Are microcracks really critical?, *ACS Energy Lett.*, 4(2019), No. 6, p. 1394.
[68] H.H. Ryu, K.J. Park, C.S. Yoon, and Y.K. Sun, Capacity fading of Ni-rich $Li[Ni_xCo_yMn_{1-x-y}]O_2$ ($0.6 \le x \le 0.95$) cathodes for high-energy-density lithium-ion batteries: Bulk or surface degradation?, *Chem. Mater.*, 30(2018), No. 3, p. 1155.
[69] A. Manthiram, A.V. Murugan, A. Sarkar, and T. Muraliganth, Nanostructured electrode materials for electrochemical energy storage and conversion, *Energy Environ. Sci.*, 1(2008), No. 6, p. 621.
[70] I. Nakai, K. Takahashi, Y. Shiraishi, T. Nakagome, and F. Nishikawa, Study of the Jahn-Teller distortion in $LiNiO_2$, a cathode material in a rechargeable lithium battery, by *in situ* X-ray absorption fine structure analysis, *J. Solid State Chem.*,

140(1998), No. 1, p. 145.
[71] P. Kalyani and N. Kalaiselvi, Various aspects of $LiNiO_2$ chemistry: A review, *Sci. Technol. Adv. Mater.*, 6(2005), No. 6, p. 689.
[72] A. Rougier, I. Saadoune, P. Gravereau, P. Willmann, and C. Delmasa, Effect of cobalt substitution on cationic distribution in $LiNi_{1-y}Co_yO_2$ electrode materials, *Solid State Ionics*, 90(1996), No. 1-4, p. 83.
[73] Z.H. Lu, D.D. MacNeil, and J.R. Dahn, Layered $Li[Ni_xCo_{1-2x}Mn_x]O_2$ cathode materials for lithium-ion batteries, *Electrochem. Solid-State Lett.*, 4(2001), No. 12, p. A200.
[74] U.H. Kim, L.Y. Kuo, P. Kaghazchi, C.S. Yoon, and Y.K. Sun, Quaternary layered Ni-rich NCMA cathode for lithium-ion batteries, *ACS Energy Lett.*, 4(2019), No. 2, p. 576.
[75] K. Kang and G. Ceder, Factors that affect Li mobility in layered lithium transition metal oxides, *Phys. Rev. B*, 74(2006), No. 9, art. No. 094105.
[76] R.R. Zhao, Z.L. Yang, J.X. Liang, *et al*., Understanding the role of Na-doping on Ni-rich layered oxide $LiNi_{0.5}Co_{0.2}Mn_{0.3}O_2$, *J. Alloys Compd.*, 689(2016), p. 318.
[77] T. He, L. Chen, Y.F. Su, *et al*., The effects of alkali metal ions with different ionic radii substituting in Li sites on the electrochemical properties of Ni-rich cathode materials, *J. Power Sources*, 441(2019), art. No. 227195.
[78] Z.C. Ye, L. Qiu, W. Yang, *et al*., Nickel-rich layered cathode materials for lithium-ion batteries, *Chemistry*, 27(2021), No. 13, p. 4249.
[79] R.P. Qing, J.L. Shi, D.D. Xiao, *et al*., Enhancing the kinetics of Li-rich cathode materials through the pinning effects of gradient surface Na^+ doping, *Adv. Energy Mater.*, 6(2016), No. 6, art. No. 1501914.
[80] M.M. Chen, E.Y. Zhao, D.F. Chen, *et al*., Decreasing Li/Ni disorder and improving the electrochemical performances of Ni-rich $LiNi_{0.8}Co_{0.1}Mn_{0.1}O_2$ by Ca doping, *Inorg. Chem.*, 56(2017), No. 14, p. 8355.
[81] K. Kang, Y.S. Meng, J. Breger, C.P. Grey, and G. Ceder, Electrodes with high power and high capacity for rechargeable lithium batteries, *ChemInform*, 311(2006), No. 5763, p. 977.
[82] E.J. Wu, P.D. Tepesch, and G. Ceder, Size and charge effects on the structural stability of $LiMO_2$ (M=transition metal) compounds, *Philos. Mag. B*, 77(1998), No. 4, p. 1039.
[83] L.S. Ni, H.Y. Chen, J.Q. Gao, *et al*., Calcium-induced pinning effect for high-performance Co-free Ni-rich NMA layered cathode, *Nano Energy*, 115(2023), art. No. 108743.
[84] A. Rajkamal and H. Kim, Formation of pillar-ions in the Li layer decreasing the Li/Ni disorder and improving the structural stability of cation-doped Ni-rich $LiNi_{0.8}Co_{0.1}Mn_{0.1}O_2$: A first-principles verification, *ACS Appl. Energy Mater.*, 4(2021), No. 12, p. 14068.
[85] Y.D. Zhang, J.D. Liu, W.C. Xu, *et al*., Gradient doping Mg and Al to stabilize Ni-rich cathode materials for rechargeable lithium-ion batteries, *J. Power Sources*, 535(2022), art. No. 231445.
[86] H.F. Yu, H.W. Zhu, Z.F. Yang, M.M. Liu, H. Jiang, and C.Z. Li, Bulk Mg-doping and surface polypyrrole-coating enable high-rate and long-life for Ni-rich layered cathodes, *Chem. Eng. J.*, 412(2021), art. No. 128625.
[87] C.L. Xu, W. Xiang, Z.G. Wu, *et al*., Dual-site lattice modification regulated cationic ordering for Ni-rich cathode towards boosted structural integrity and cycle stability, *Chem. Eng. J.*, 403(2021), art. No. 126314.
[88] A. D'Epifanio, F. Croce, F. Ronci, V. Rossi Albertini, E. Traversa, and B. Scrosati, Effect of Mg^{2+} doping on the structural, thermal, and electrochemical properties of $LiNi_{0.8}Co_{0.16}Mg_{0.04}O_2$, *Chem. Mater.*, 16(2004), No. 18, p. 3559.
[89] C. Pouillerie, F. Perton, P. Biensan, J.P. Pérès, M. Broussely, and C. Delmas, Effect of magnesium substitution on the cycling behavior of lithium nickel cobalt oxide, *J. Power Sources*, 96(2001), No. 2, p. 293.
[90] J.S. Kim, S. Lim, H. Munakata, S.S. Kim, and K. Kanamura, Understanding the relationship of electrochemical properties and structure of microstructure-controlled core shell gradient type Ni-rich cathode material by single particle measurement, *Electrochim. Acta*, 390(2021), art. No. 138813.
[91] C.C. Chang, J.Y. Kim, and P.N. Kumta, Synthesis and electrochemical characterization of divalent cation-incorporated lithium nickel oxide, *J. Electrochem. Soc.*, 147(2000), No. 5, p. 1722.
[92] B. Ammundsen, J. Paulsen, I. Davidson, *et al*., Local structure and first cycle redox mechanism of layered $Li_{1.2}Cr_{0.4}Mn_{0.4}O_2$ cathode material, *J. Electrochem. Soc.*, 149(2002), No. 4, p. A431.
[93] L.J. Li, Z.X. Wang, Q.C. Liu, C. Ye, Z.Y. Chen, and L. Gong, Effects of chromium on the structural, surface chemistry and electrochemical of layered $LiNi_{0.8-x}Co_{0.1}Mn_{0.1}Cr_xO_2$, *Electrochim. Acta*, 77(2012), p. 89.
[94] C.X. Zhang, S. Xu, B. Han, *et al*., Towards rational design of high performance Ni-rich layered oxide cathodes: The interplay of borate-doping and excess lithium, *J. Power Sources*, 431(2019), p. 40.
[95] L.C. Pan, Y.G. Xia, B. Qiu, *et al*., Structure and electrochemistry of B doped $Li(Li_{0.2}Ni_{0.13}Co_{0.13}Mn_{0.54})_{1-x}B_xO_2$ as cathode materials for lithium-ion batteries, *J. Power Sources*, 327(2016), p. 273.
[96] K.J. Park, H.G. Jung, L.Y. Kuo, P. Kaghazchi, C.S. Yoon, and Y.K. Sun, Improved cycling stability of $Li[Ni_{0.90}Co_{0.05}Mn_{0.05}]O_2$ through microstructure modification by boron doping for Li-ion batteries, *Adv. Energy Mater.*, 8(2018), No. 25, art. No. 1801202.
[97] X. Liu, G.L. Xu, L. Yin, *et al*., Probing the thermal-driven structural and chemical degradation of Ni-rich layered cathodes by Co/Mn exchange, *J. Am. Chem. Soc.*, 142(2020), No. 46, p. 19745.
[98] W.W. Yan, S.Y. Yang, Y.Y. Huang, Y. Yang, and G.H. Yuan, A review on doping/coating of nickel-rich cathode materials for lithium-ion batteries, *J. Alloys Compd.*, 819(2020), art. No. 153048.
[99] F.X. Xin, H. Zhou, Y.X. Zong, *et al*., What is the role of Nb in nickel-rich layered oxide cathodes for lithium-ion batteries?, *ACS Energy Lett.*, 6(2021), No. 4, p. 1377.
[100] B. Wang, H.L. Zhao, F.P. Cai, *et al*., Surface engineering with ammonium niobium oxalate: A multifunctional strategy to enhance electrochemical performance and thermal stability of Ni-rich cathode materials at 4.5V cutoff potential, *Electrochim. Acta*, 403(2022), art. No. 139636.
[101] M. Wang, Y.Q. Han, M. Chu, L. Chen, M. Liu, and Y.J. Gu, Enhanced electrochemical performances of cerium-doped Li-Rich $Li_{1.2}Ni_{0.13}Co_{0.13}Mn_{0.54}O_2$ cathode materials, *J. Alloys Compd.*, 861(2021), art. No. 158000.
[102] T. Thien Nguyen, U.H. Kim, C.S. Yoon, and Y.K. Sun, Enhanced cycling stability of Sn-doped $Li[Ni_{0.90}Co_{0.05}Mn_{0.05}]O_2$ via optimization of particle shape and orientation, *Chem. Eng. J.*, 405(2021), art. No. 126887.
[103] L. Cheng, Y.N. Zhou, B. Zhang, *et al*., High-rate Ni-rich single-crystal cathodes with highly exposed {010} active planes through *in-situ* Zr doping, *Chem. Eng. J.*, 452(2023), art. No. 139336.
[104] B. Wang, F.P. Cai, C.X. Chu, *et al*., Modification of the Ni-rich layered cathode material by Hf addition: Synergistic microstructural engineering and surface stabilization, *ACS Appl. Mater. Interfaces*, 16(2024), No. 10, p. 12599.
[105] S.Q. Liu, B.Y. Wang, X. Zhang, S. Zhao, Z.H. Zhang, and H.J. Yu, Reviving the lithium-manganese-based layered oxide cath-

odes for lithium-ion batteries, *Matter*, 4(2021), No. 5, p. 1511.
[106] X. Li, W.J. Ge, K.K. Zhang, G.C. Peng, Y.X. Fu, and X.G. Ma, Comprehensive study of tantalum doping on morphology, structure, and electrochemical performance of Ni-rich cathode materials, *Electrochim. Acta*, 403(2022), art. No. 139653.
[107] C.X. Mei, F.H. Du, L. Wu, *et al*., Stabilization of crystal and interfacial structure of Ni-rich cathode material by vanadium-doping, *J. Colloid Interface Sci.*, 617(2022), p. 193.
[108] Z.P. Qiu, Y.L. Zhang, Z. Liu, Y. Gao, J.M. Liu, and Q.G. Zeng, Stabilizing Ni-rich $LiNi_{0.92}Co_{0.06}Al_{0.02}O_2$ cathodes by boracic polyanion and tungsten cation co-doping for high-energy lithium-ion batteries, *ChemElectroChem*, 7(2020), No. 18, p. 3811.
[109] T. Sattar, S.H. Lee, B.S. Jin, and H.S. Kim, Influence of Mo addition on the structural and electrochemical performance of Ni-rich cathode material for lithium-ion batteries, *Sci. Rep.*, 10(2020), No. 1, art. No. 8562.
[110] A. Gomez-Martin, F. Reissig, L. Frankenstein, *et al*., Magnesium substitution in Ni-rich NMC layered cathodes for high-energy lithium ion batteries, *Adv. Energy Mater.*, 12(2022), No. 8, art. No. 2103045.
[111] H.H. Sun, T.P. Pollard, O. Borodin, K. Xu, and J.L. Allen, Degradation of high nickel Li-ion cathode materials induced by exposure to fully-charged state and its mitigation, *Adv. Energy Mater.*, 13(2023), No. 18, art. No. 2204360.
[112] G.T. Park, B. Namkoong, S.B. Kim, J. Liu, C.S. Yoon, and Y.K. Sun, Introducing high-valence elements into cobalt-free layered cathodes for practical lithium-ion batteries, *Nat. Energy*, 7(2022), p. 946.
[113] X.Y. Zhang, P.P. Zhang, T.Y. Zeng, *et al*., Improving the structure stability of $LiNi_{0.8}Co_{0.15}Al_{0.05}O_2$ by double modification of tantalum surface coating and doping, *ACS Appl. Energy Mater.*, 4(2021), No. 8, p. 8641.
[114] L.S. Li, Z. Zhang, S.H. Fu, and Z.Z. Liu, F127-assisted synthesis of $LiNi_{0.5}Co_{0.2}Mn_{0.3}O_{1.99}F_{0.01}$ as a high rate and long lifespan cathode material for lithium-ion batteries, *Appl. Surf. Sci.*, 476(2019), p. 1061.
[115] X.L. Liu, S. Wang, L. Wang, *et al*., Stabilizing the high-voltage cycle performance of $LiNi_{0.8}Co_{0.1}Mn_{0.1}O_2$ cathode material by Mg doping, *J. Power Sources*, 438(2019), art. No. 227017.
[116] Z.H. Cui, Q. Xie, and A. Manthiram, Zinc-doped high-nickel, low-cobalt layered oxide cathodes for high-energy-density lithium-ion batteries, *ACS Appl. Mater. Interfaces*, 13(2021), No. 13, p. 15324.
[117] H. Gu, Y. Mu, S.T. Zhang, *et al*., Enhanced thermal safety and rate capability of nickel-rich cathodes via optimal Nb-doping strategy, *Electrochim. Acta*, 487(2024), art. No. 144216.
[118] N.Y. Park, G. Cho, S.B. Kim, and Y.K. Sun, Multifunctional doping strategy to develop high-performance Ni-rich cathode material, *Adv. Energy Mater.*, 13(2023), No. 14, art. No. 2204291.
[119] H.H. Ryu, H.W. Lim, S.G. Lee, and Y.K. Sun, Optimization of molybdenum-doped Ni-rich layered cathodes for long-term cycling, *Energy Storage Mater.*, 59(2023), art. No. 102771.
[120] R. Zhang, C.Y. Wang, P.C. Zou, *et al*., Compositionally complex doping for zero-strain zero-cobalt layered cathodes, *Nature*, 610(2022), No. 7930, p. 67.
[121] B.K. Yu, Y.Q. Wang, J.Q. Li, *et al*., Recent advances on low-Co and Co-free high entropy layered oxide cathodes for lithium-ion batteries, *Nanotechnology*, 34(2023), No. 45, art. No. 452501.
[122] J.B. Wang, Y.Y. Cui, Q.S. Wang, *et al*., Lithium containing layered high entropy oxide structures, *Sci. Rep.*, 10(2020), No. 1, art. No. 18430.
[123] J. Sturman, C.H. Yim, E.A. Baranova, and Y. Abu-Lebdeh, Communication—Design of $LiNi_{0.2}Mn_{0.2}Co_{0.2}Fe_{0.2}Ti_{0.2}O_2$ as a high-entropy cathode for lithium-ion batteries guided by machine learning, *J. Electrochem. Soc.*, 168(2021), No. 5, art. No. 050541.
[124] K.D. Wang, K. Nishio, K. Horiba, *et al*., Synthesis of high-entropy layered oxide epitaxial thin films: $LiCr_{1/6}Mn_{1/6}Fe_{1/6}Co_{1/6}Ni_{1/6}Cu_{1/6}O_2$, *Cryst. Growth Des.*, 22(2022), No. 2, p. 1116.
[125] T. Kawaguchi, X. Bian, T. Hatakeyama, H.Y. Li, and T. Ichitsubo, Influences of enhanced entropy in layered rocksalt oxide cathodes for lithium-ion batteries, *ACS Appl. Energy Mater.*, 5(2022), No. 4, p. 4369.
[126] J. Song, F.H. Ning, Y.X. Zuo, *et al*., Entropy stabilization strategy for enhancing the local structural adaptability of Li-rich cathode materials, *Adv. Mater.*, 35(2023), No. 7, art. No. 2208726.
[127] Z.Y. Lun, B. Ouyang, D.H. Kwon, *et al*., Cation-disordered rocksalt-type high-entropy cathodes for Li-ion batteries, *Nat. Mater.*, 20(2021), No. 2, p. 214.
[128] S.Y. Zhou, Y.X. Sun, T. Gao, J.H. Liao, S.X. Zhao, and G.Z. Cao, Enhanced Li^+ diffusion and lattice oxygen stability by the high entropy effect in disordered-rocksalt cathodes, *Angew. Chem. Int. Ed.*, 62(2023), No. 42, art. No. e202311930.
[129] X.Y. Zhao and G. Ceder, Zero-strain cathode materials for Li-ion batteries, *Joule*, 6(2022), No. 12, p. 2683.
[130] X.Y. Zhao, Y.S. Tian, Z.Y. Lun, *et al*., Design principles for zero-strain Li-ion cathodes, *Joule*, 6(2022), No. 7, p. 1654.
[131] I. Konuma, D. Goonetilleke, N. Sharma, *et al*., A near dimensionally invariable high-capacity positive electrode material, *Nat. Mater.*, 22(2023), No. 2, p. 225.
[132] A. Bano, M. Noked, and D.T. Major, Theoretical insights into high-entropy Ni-rich layered oxide cathodes for low-strain Li-ion batteries, *Chem. Mater.*, 35(2023), No. 20, p. 8426.
[133] D.C. Chen, J. Ahn, and G.Y. Chen, An overview of cation-disordered lithium-excess rocksalt cathodes, *ACS Energy Lett.*, 6(2021), No. 4, p. 1358.
[134] R.J. Clément, Z. Lun, and G. Ceder, Cation-disordered rocksalt transition metal oxides and oxyfluorides for high energy lithium-ion cathodes, *Energy Environ. Sci.*, 13(2020), No. 2, p. 345.
[135] K. Zhou, Y.N. Li, Y. Ha, *et al*., A nearly zero-strain Li-rich rock-salt oxide with multielectron redox reactions as a cathode for Li-ion batteries, *Chem. Mater.*, 34(2022), No. 21, p. 9711.
[136] J. Lee, A. Urban, X. Li, D. Su, G. Hautier, and G. Ceder, Unlocking the potential of cation-disordered oxides for rechargeable lithium batteries, *Science*, 343(2014), No. 6170, p. 519.
[137] M. Nakajima and N. Yabuuchi, Lithium-excess cation-disordered rocksalt-type oxide with nanoscale phase segregation: $Li_{1.25}Nb_{0.25}V_{0.5}O_2$, *Chem. Mater.*, 29(2017), No. 16, p. 6927.
[138] R.J. Qi, I. Konuma, B.D.L. Campéon, Y. Kaneda, M. Kondo, and N. Yabuuchi, Highly graphitic carbon coating on $Li_{1.25}Nb_{0.25}V_{0.5}O_2$ derived from a precursor with a perylene core for high-power battery applications, *Chem. Mater.*, 34(2022), No. 4, p. 1946.
[139] C. Zhan, T.P. Wu, J. Lu, and K. Amine, Dissolution, migration, and deposition of transition metal ions in Li-ion batteries exemplified by Mn-based cathodes–A critical review, *Energy Environ. Sci.*, 11(2018), No. 2, p. 243.
[140] W.S. Li, Review—An unpredictable hazard in lithium-ion batteries from transition metal ions: Dissolution from cathodes, deposition on anodes and elimination strategies, *J. Electrochem. Soc.*, 167(2020), No. 9, art. No. 090514.
[141] G.J. Ross, J.F. Watts, M.P. Hill, and P. Morrissey, Surface modification of poly(vinylidene fluoride) by alkaline treatment 1. The degradation mechanism, *Polymer*, 41(2000), No. 5, p. 1685.
[142] Y. You, H. Celio, J.Y. Li, A. Dolocan, and A. Manthiram,

Modified high-nickel cathodes with stable surface chemistry against ambient air for lithium-ion batteries, *Angew. Chem. Int. Ed.*, 57(2018), No. 22, p. 6480.
[143] M.J. Herzog, N. Gauquelin, D. Esken, J. Verbeeck, and J. Janek, Facile dry coating method of high-nickel cathode material by nanostructured fumed alumina (Al_2O_3) improving the performance of lithium-ion batteries, *Energy Technol.*, 9(2021), No. 4, art. No. 2100028.
[144] D.Z. Hu, Y.F. Su, L. Chen, *et al*., The mechanism of side reaction induced capacity fading of Ni-rich cathode materials for lithium ion batteries, *J. Energy Chem.*, 58(2021), p. 1.
[145] L.T. Dou, P. Hu, C.Q. Shang, *et al*., Enhanced electrochemical performance of $LiNi_{0.8}Co_{0.1}Mn_{0.1}O_2$ with SiO_2 surface coating via homogeneous precipitation, *ChemElectroChem*, 8(2021), No. 22, p. 4321.
[146] Y.Y. Li, X.F. Li, J.H. Hu, *et al*., ZnO interface modified $LiNi_{0.6}Co_{0.2}Mn_{0.2}O_2$ toward boosting lithium storage, *Energy Environ. Mater.*, 3(2020), No. 4, p. 522.
[147] Q.L. Fan, K.J. Lin, S.D. Yang, *et al*., Constructing effective TiO_2 nano-coating for high-voltage Ni-rich cathode materials for lithium ion batteries by precise kinetic control, *J. Power Sources*, 477(2020), art. No. 228745.
[148] Y.R. Bak, Y. Chung, J.H. Ju, M.J. Hwang, Y. Lee, and K.S. Ryu, Structure and electrochemical performance of $LiNi_{0.8}Co_{0.15}Al_{0.05}O_2$ cathodes before and after treatment with $Co_3(PO_4)_2$ or $AlPO_4$ by *in situ* chemical method, *J. New Mater. Electrochem. Syst.*, 14(2011), No. 4, p. 203.
[149] D.J. Lee, B. Scrosati, and Y.K. Sun, $Ni_3(PO_4)_2$-coated $Li[Ni_{0.8}Co_{0.15}Al_{0.05}]O_2$ lithium battery electrode with improved cycling performance at 55°C, *J. Power Sources*, 196(2011), No. 18, p. 7742.
[150] Y.Q. Chu, Y.B. Mu, L.F. Zou, *et al*., Thermodynamically stable dual-modified LiF&FeF_3 layer empowering Ni-rich cathodes with superior cyclabilities, *Adv. Mater.*, 35(2023), No. 21, art. No. 2212308.
[151] G.R. Hu, X.Y. Qi, K.H. Hu, *et al*., A facile cathode design with a $LiNi_{0.6}Co_{0.2}Mn_{0.2}O_2$ core and an AlF_3-activated $Li_{1.2}Ni_{0.2}Mn_{0.6}O_2$ shell for Li-ion batteries, *Electrochim. Acta*, 265(2018), p. 391.
[152] K.S. Ryu, S.H. Lee, and Y.J. Park, Electrochemical properties of $LiNi_{0.8}Co_{0.16}Al_{0.04}O_2$ and surface modification with $Co_3(PO_4)_2$ as cathode materials for lithium battery, *Bull. Korean Chem. Soc.*, 29(2008), No. 9, p. 1737.
[153] Z.K. Zhao, S. Chen, D.B. Mu, *et al*., Understanding the surface decoration on primary particles of nickel-rich layered $LiNi_{0.6}Co_{0.2}Mn_{0.2}O_2$ cathode material with lithium phosphate, *J. Power Sources*, 431(2019), p. 84.
[154] Q.M. Gan, N. Qin, Z.Y. Wang, *et al*., Revealing mechanism of Li_3PO_4 coating suppressed surface oxygen release for commercial Ni-rich layered cathodes, *ACS Appl. Energy Mater.*, 3(2020), No. 8, p. 7445.
[155] J.L. Fu, D.B. Mu, B.R. Wu, *et al*., Enhanced electrochemical performance of $LiNi_{0.6}Co_{0.2}Mn_{0.2}O_2$ cathode at high cutoff voltage by modifying electrode/electrolyte interface with lithium metasilicate, *Electrochim. Acta*, 246(2017), p. 27.
[156] D. Wang, X.H. Li, Z.X. Wang, *et al*., Multifunctional Li_2O–$2B_2O_3$ coating for enhancing high voltage electrochemical performances and thermal stability of layered structured $LiNi_{0.5}Co_{0.2}Mn_{0.3}O_2$ cathode materials for lithium ion batteries, *Electrochim. Acta*, 174(2015), p. 1225.
[157] C.C. Zhang, S.Y. Liu, J.M. Su, *et al*., Revealing the role of NH_4VO_3 treatment in Ni-rich cathode materials with improved electrochemical performance for rechargeable lithium-ion batteries, *Nanoscale*, 10(2018), No. 18, p. 8820.
[158] M.H. Park, M. Noh, S.H. Lee, *et al*., Flexible high-energy Li-ion batteries with fast-charging capability, *Nano Lett.*, 14(2014), No. 7, p. 4083.
[159] K. Sahni, M. Ashuri, Q.R. He, *et al*., H_3PO_4 treatment to enhance the electrochemical properties of $Li(Ni_{1/3}Mn_{1/3}Co_{1/3})O_2$ and $Li(Ni_{0.5}Mn_{0.3}Co_{0.2})O_2$ cathodes, *Electrochim. Acta*, 301(2019), p. 8.
[160] X.H. Xiong, D. Ding, Y.F. Bu, *et al*., Enhanced electrochemical properties of a $LiNiO_2$-based cathode material by removing lithium residues with $(NH_4)_2HPO_4$, *J. Mater. Chem. A*, 2(2014), No. 30, p. 11691.
[161] G. Kaur and B.D. Gates, Review-surface coatings for cathodes in lithium ion batteries: From crystal structures to electrochemical performance, *J. Electrochem. Soc.*, 169(2022), No. 4, art. No. 043504.
[162] X.Y. Qu, H. Huang, T. Wan, *et al*., An integrated surface coating strategy to enhance the electrochemical performance of nickel-rich layered cathodes, *Nano Energy*, 91(2022), art. No. 106665.
[163] L.F. Wang, G.C. Liu, R. Wang, *et al*., Regulating surface oxygen activity by perovskite-coating-stabilized ultrahigh-nickel layered oxide cathodes, *Adv. Mater.*, 35(2023), No. 11, art. No. 2209483.
[164] H. Sheng, X.H. Meng, D.D. Xiao, *et al*., An air-stable high-nickel cathode with reinforced electrochemical performance enabled by convertible amorphous Li_2CO_3 modification, *Adv. Mater.*, 34(2022), No. 12, art. No. 2108947.
[165] Y.B. Shen, X.Y. Zhang, L.C. Wang, *et al*., A universal multifunctional rare earth oxide coating to stabilize high-voltage lithium layered oxide cathodes, *Energy Storage Mater.*, 56(2023), p. 155.
[166] X.Y. Zheng, R.H. Yu, J. Sun, *et al*., Precursor-oriented ultrathin Zr-based gradient coating on Ni-riched cathodes, *Nano Energy*, 105(2023), art. No. 108000.
[167] Z.H. Chen, Y. Qin, K. Amine, and Y.K. Sun, Role of surface coating on cathode materials for lithium-ion batteries, *J. Mater. Chem.*, 20(2010), No. 36, p. 7606.
[168] J.H. Shim, Y.M. Kim, M. Park, J. Kim, and S.H. Lee, Reduced graphene oxide-wrapped nickel-rich cathode materials for lithium ion batteries, *ACS Appl. Mater. Interfaces*, 9(2017), No. 22, p. 18720.
[169] Y. Yoon, S. Shin, and M.W. Shin, Fundamental understanding of the effect of a polyaniline coating layer on cation mixing and chemical states of $LiNi_{0.9}Co_{0.085}Mn_{0.015}O_2$ for Li-ion batteries, *ACS Appl. Polym. Mater.*, 5(2023), No. 2, p. 1344.
[170] B.Z. You, Z.X. Wang, F. Shen, *et al*., Research progress of single-crystal nickel-rich cathode materials for lithium ion batteries, *Small Meth.*, 5(2021), No. 8, art. No. 2100234.
[171] H. Huang, L.P. Zhang, H.Y. Tian, *et al*., Pulse high temperature sintering to prepare single-crystal high nickel oxide cathodes with enhanced electrochemical performance, *Adv. Energy Mater.*, 13(2023), No. 3, art. No. 2203188.
[172] A.H. Ran, S.X. Chen, M. Cheng, *et al*., A single-crystal nickel-rich material as a highly stable cathode for lithium-ion batteries, *J. Mater. Chem. A*, 10(2022), No. 37, p. 19680.
[173] J.T. Hu, L.Z. Li, Y.J. Bi, *et al*., Locking oxygen in lattice: A quantifiable comparison of gas generation in polycrystalline and single crystal Ni-rich cathodes, *Energy Storage Mater.*, 47(2022), p. 195.
[174] X.B. Kong, Y.G. Zhang, J.Y. Li, *et al*., Single-crystal structure helps enhance the thermal performance of Ni-rich layered cathode materials for lithium-ion batteries, *Chem. Eng. J.*, 434(2022), art. No. 134638.
[175] A. Neubrand and J. Rödel, Gradient materials: An overview of a novel concept, *Int. J. Mater. Res.*, 88(2021), No. 5, p. 358.
[176] P.Y. Hou, H.Z. Zhang, Z.Y. Zi, L.Q. Zhang, and X.J. Xu, Core–shell and concentration-gradient cathodes prepared *via* co-precipitation reaction for advanced lithium-ion batteries, *J. Mater. Chem. A*, 5(2017), No. 9, p. 4254.
[177] R. Lin, S.M. Bak, Y. Shin, *et al*., Hierarchical nickel valence

gradient stabilizes high-nickel content layered cathode materials, *Nat. Commun.*, 12(2021), No. 1, art. No. 2350.
[178] A. Purwanto, C.S. Yudha, U. Ubaidillah, H. Widiyandari, T. Ogi, and H. Haerudin, NCA cathode material: Synthesis methods and performance enhancement efforts, *Mater. Res. Express*, 5(2018), No. 12, art. No. 122001.
[179] D. Aurbach, K. Gamolsky, B. Markovsky, Y. Gofer, M. Schmidt, and U. Heider, On the use of vinylene carbonate (VC) as an additive to electrolyte solutions for Li-ion batteries, *Electrochim. Acta*, 47(2002), No. 9, p. 1423.
[180] R. Dugas, A. Ponrouch, G. Gachot, R. David, M.R. Palacin, and J.M. Tarascon, Na reactivity toward carbonate-based electrolytes: The effect of FEC as additive, *J. Electrochem. Soc.*, 163(2016), No. 10, p. A2333.
[181] R. Sahore, A. Tornheim, C. Peebles, *et al*., Methodology for understanding interactions between electrolyte additives and cathodes: A case of the tris(2, 2, 2-trifluoroethyl)phosphite additive, *J. Mater. Chem. A*, 6(2018), No. 1, p. 198.
[182] A. Hofmann, M. Migeot, E. Thißen, *et al*., Electrolyte mixtures based on ethylene carbonate and dimethyl sulfone for Li-ion batteries with improved safety characteristics, *ChemSusChem*, 8(2015), No. 11, p. 1892.
[183] K. Beltrop, S. Klein, R. Nölle, *et al*., Triphenylphosphine oxide as highly effective electrolyte additive for graphite/NMC811 lithium ion cells, *Chem. Mater.*, 30(2018), No. 8, p. 2726.
[184] B.W. Deng, H. Wang, X. Li, *et al*., Effects of charge cutoff potential on an electrolyte additive for $LiNi_{0.6}Co_{0.2}Mn_{0.2}O_2$–mesocarbon microbead full cells, *Energy Technol.*, 7(2019), No. 4, art. No. 1800981.
[185] Z.Y. Luo, H. Zhang, L. Yu, D.H. Huang, and J.Q. Shen, Improving long-term cyclic performance of $LiNi_{0.8}Co_{0.15}Al_{0.05}O_2$ cathode by introducing a film forming additive, *J. Electroanal. Chem.*, 833(2019), p. 520.
[186] H.Q. Pham, Y.H. Thi Tran, J. Han, and S.W. Song, Roles of nonflammable organic liquid electrolyte in stabilizing the interface of the $LiNi_{0.8}Co_{0.1}Mn_{0.1}O_2$ cathode at 4.5 V and improving the battery performance, *J. Phys. Chem. C*, 124(2020), No. 1, p. 175.
[187] Y.M. Lee, K.M. Nam, E.H. Hwang, *et al*., Interfacial origin of performance improvement and fade for 4.6 V $LiNi_{0.5}Co_{0.2}Mn_{0.3}O_2$ battery cathodes, *J. Phys. Chem. C*, 118(2014), No. 20, p. 10631.
[188] Y. Han, S.H. Jung, H. Kwak, *et al*., Single- or poly-crystalline Ni-rich layered cathode, sulfide or halide solid electrolyte: Which will be the winners for all-solid-state batteries?, *Adv. Energy Mater.*, 11(2021), No. 21, art. No. 2100126.
[189] W. Jiang, X.X. Zhu, R.Z. Huang, *et al*., Revealing the design principles of Ni-rich cathodes for all-solid-state batteries, *Adv. Energy Mater.*, 12(2022), No. 13, art. No. 2103473.
[190] S.H. Jung, U.H. Kim, J.H. Kim, *et al*., Ni-rich layered cathode materials with electrochemo-mechanically compliant microstructures for all-solid-state Li batteries, *Adv. Energy Mater.*, 10(2020), No. 6, art. No. 1903360.
[191] L.S. Li, H.H. Duan, J. Li, L. Zhang, Y.F. Deng, and G.H. Chen, Toward high performance all-solid-state lithium batteries with high-voltage cathode materials: Design strategies for solid electrolytes, cathode interfaces, and composite electrodes, *Adv. Energy Mater.*, 11(2021), No. 28, art. No. 2003154.
[192] X.S. Liu, B.Z. Zheng, J. Zhao, *et al*., Electrochemo-mechanical effects on structural integrity of Ni-rich cathodes with different microstructures in all solid-state batteries, *Adv. Energy Mater.*, 11(2021), No. 8, art. No. 2003583.
[193] Y. Ma, J.H. Teo, F. Walther, *et al*., Advanced nanoparticle coatings for stabilizing layered Ni-rich oxide cathodes in solid-state batteries, *Adv. Funct. Mater.*, 32(2022), No. 23, art. No. 2111829.
[194] S.X. Deng, X. Li, Z.H. Ren, *et al*., Dual-functional interfaces for highly stable Ni-rich layered cathodes in sulfide all-solid-state batteries, *Energy Storage Mater.*, 27(2020), p. 117.